Effect of organic compounds on the retention of radionuclides in clay rocks: Mechanisms and specificities of Eu(III), Th(IV), and U(VI)

Lizaveta Fralova, Grégory Lefèvre, Benoît Madé, Remi Marsac, Emilie Thory, Romain V H Dagnelie

Effect of organic compounds on the retention of radionuclides in clay rocks: Mechanisms and specificities of Eu(III), Th(IV), and U(VI)

Lizaveta Fralova[a], Grégory Lefèvre[b], Benoît Madé[c],

Rémi Marsac[d], Emilie Thory[a], Romain V.H. Dagnelie[a,*]

[a] Université Paris-Saclay, CEA, Service d'Étude du Comportement des Radionucléides, 91191, Gif-sur-Yvette, France

[b] PSL Research University, Chimie ParisTech-CNRS, Institut de Recherche de Chimie Paris, 11 rue Pierre et Marie Curie, F-75005 Paris, France

[c] Andra, R&D Division, parc de la Croix Blanche, 92298, Châtenay-Malabry, France

[d] Univ. Rennes, CNRS, Géosciences Rennes - UMR 6118, F-35000, Rennes, France

* Corresponding author. Université Paris-Saclay, CEA/DES/ISAS/DPC/SECR/L3MR, 91191, Gif-sur-Yvette, France.

E-mail address: romain.dagnelie@cea.fr

Abstract

The use of geological barriers is widely studied in the context of hazardous waste management and pollution events. In the near field of pollution sources, geological barriers endure disturbances with the concomitant release of hazardous chemicals and organic or saline plumes. In this study, we investigate the effect of organic compounds on the retention of radionuclides in contact with a sedimentary rock, namely Callovo-Oxfordian clay rock (East of Paris Basin). The retention of Eu(III), Th(IV), U(VI), was quantified at near-neutral pH, in presence of model organic compounds released from wastes and engineered barriers, e.g. ortho-phthalate, α-isosaccharinate (α-ISA), succinate, as well as high complexing compounds (oxalate, citrate, EDTA). The studied concentrations of organic compounds, eventually higher than disposal conditions, aimed at quantifying concentration ranges above which the retention of radionuclides decreases, and the underlying mechanisms occurring.

A simplified surface complexation model, assuming illite as the main sorbing phase, was used for predictive modelling. The comparison with experimental results allowed the evaluation of the robustness of the surface complexation constants and of the thermodynamic database "ThermoChimie" of the Andra-RWM-Ondraf/Niras consortium, to account for speciation in solution (ThermoChimie V10a, https://www.thermochimie-tdb.com). Specific mechanisms are discussed, such as complexation of Eu(III) by α-ISA, or retention of Th(IV) / citrate complexes. U(VI) displayed a unique behaviour because of uranyl complexation by natural species under geological conditions. The low solid to liquid distribution ratio, R_d(U(VI)/COx) ~ 7.5 ± 1.6 L kg^{-1} decreases in presence of organic compounds, but without direct complexation by organic molecules. Indeed, the organic plume induces a disturbance of chemical equilibria in pore water of the clay rock, leading to additional complexation of uranyl by calcium and carbonates. Such effect highlights the crucial role of clay surfaces and carbonate minerals. More generally, these results provide insights on the geochemical buffers and key parameters involved during near-field disturbance of environmental media.

Graphical Abstract

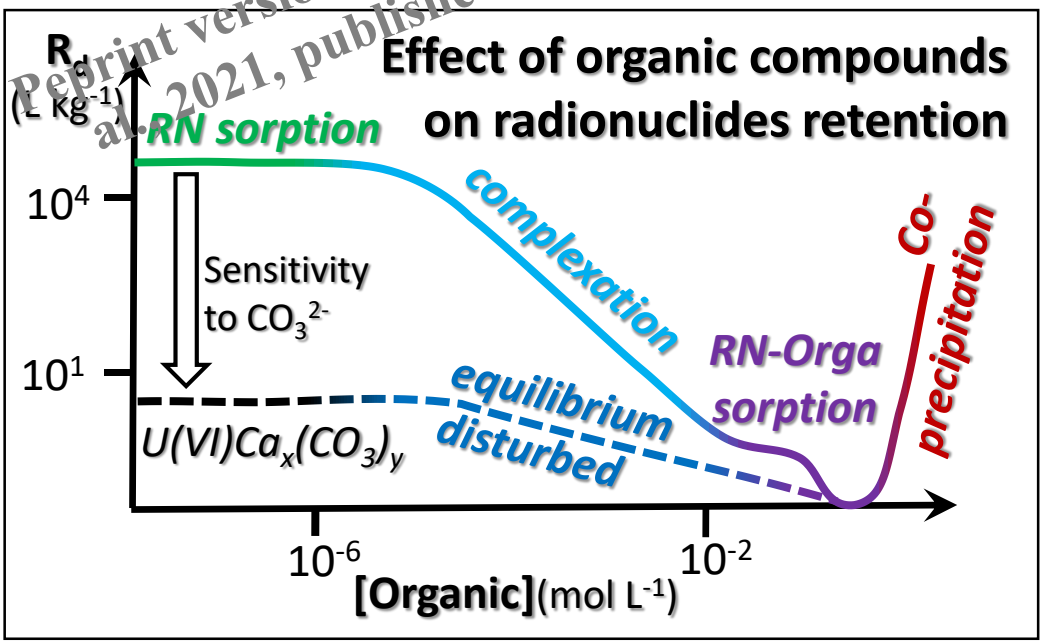

Highlights:

Retention of Eu(III), Th(IV) and U(VI) decreases in presence of organic compounds

Eu(III) and Th(IV) display various “organic concentration” sorption edges

Calcium carbonates (dis)equilibrium indirectly modifies uranyl sorption

“ThermoChimie” thermodynamic database is assessed using experimental data

1. Introduction

The knowledge of radionuclides (RNs) retention mechanisms is essential in various sectors of nuclear field, such as mining industry, environmental monitoring, and radioactive waste management (Altmann et al., 2012; Chautard et al., 2020). In the context of radioactive waste geological disposal, the French National Radioactive Waste Management Agency (Andra) is investigating natural clay rocks for their containment properties, such as Callovo-Oxfordian clayey rock (COx) (Andra, 2005; Charlet et al., 2017). The sorption of cationic species by the surfaces of clay minerals induces diffusion retardation, i.e. a decrease of their apparent diffusion coefficient by several orders of magnitude (Chen et al., 2014; Melkior et al., 2007). In contrast, anionic species display little sorption in clay rocks (Descostes et al, 2008; Dagnelie et al., 2018). The sorption parameters, i.e. solid-solution distribution coefficients, R_d (L kg^{-1}), are useful for performance assessment, in order to quantify accurately the retardation during migration of RNs.

The retention coefficients are defined for specific solution species and the retention of elements are thus highly sensitive to physico-chemical conditions (pH, Eh, temperature, salinity, etc.). Therefore, the possible evolution of the retention parameters during the transitory phases of the radioactive waste repository is an important field to assess. To this aim, the sensitivity to various effects of solid-solution distribution coefficients of RNs is evaluated , such as the presence of complexing species (McCarthy et al., 1998; Read et al., 1998), redox evolution in the far-field of disposal (Ma et al., 2019), or near-field disturbances of disposal. Dealing with near-field disturbances, the long-term degradation of engineered barriers and radioactive waste will release RNs associated with other chemicals and in few specific cases with saline and organic plumes. Therefore, numerous studies describe the complexation of RNs in presence of organic compounds, leading to an increase of solubility and a decrease of cationic species retention. Such phenomena were evidenced in presence of small organic acids (Bauer et al., 2005; Descostes et al., 2017; Tits et al., 2005) as well as larger humic acids (Dublet et al., 2017; Hongxia et al., 2016; Joseph et al., 2011; Kautenburger et al., 2019). In addition to experiments on reference solids (i.e. pure minerals), the study of chemical disturbances on natural media seems complementary, as transient phases also depend on the mineralogical assemblage of samples, the accessible surfaces, and the solid to liquid ratios (m/V) (Dagnelie et al., 2015; 2017).

In this context, this study focuses on the gathering of sorption data on different RNs: Eu(III), Th(IV) and U(VI) in presence of small organic acids on a natural sedimentary rock (COx). Organic compounds are chosen in the context of near-field disturbance of geological barriers. For example, ortho-phthalic acid (o-phthalate) is an additive potentially released by degradation of plastics (Erythropel et al., 2014), ISA is a major degradation product of cellulose (Shaw, 2013) and small complexing diacids such as oxalate or succinate potentially found in dissolved natural organic matter (D.O.M.) or released during biotic degradation (Bagnoud et al. 2016; Rout et al. 2015). The main objective is to improve the predictive modelling of the RNs retention in presence of organic complexing species in sedimentary rocks. To that aim, a sorption model developed for clay minerals was used to

account for surface complexation (Bradbury et al., 2005a), and the thermodynamic database (TDB) "ThermoChimie", developed by the consortium Andra-RWM-Ondraf, was used to account for speciation in solution. The robustness and accuracy of such modelling was checked using data in absence of organic compounds. Then, the comparison between experimental results on {Organic / RNs} systems and "predictive" model allowed the assessment of the model parameters and of the database. The use of high concentrations in organic compounds, possibly beyond the operational context with respect to radioactive waste disposal, provided a better fundamental understanding on limitations of reactive-transport models. Moreover, the use of natural samples, including several minor phases such as carbonates or natural organic matter, helped evidencing secondary mechanisms, eventually occurring during chemical disturbances in environmental media.

2. Material and methods

2.1. Rock samples and chemicals

Experiments were carried out on samples that originated from the Callovo-Oxfordian sedimentary formation (East of Paris Basin, Meuse/Haute-Marne, France). The rock cores (Table S1) were drilled from a borehole in the underground laboratory at -501 m and -498 m in depth. These samples come from the clayey unit constituted of 30-55% clay minerals (illite, interlayered illite-smectite (I/S), kaolinite, chlorite), 18-20% tectosilicates (mainly quartz), 22-35% carbonate minerals (mainly calcite, dolomite), < 5% accessory minerals (pyrite, iron oxi-hydroxide etc.) and ~ 0.6% organic matter (Gaucher et al., 2004; Lerouge et al., 2011; Pellenard and Deconinck, 2006). The measure of cationic exchange capacity (CEC) indicated proportions of illite (~20%) and of interstratified I/S (21%). This led to a rough estimate of 30.5 ± 1% of illite, considering I/S as a mixture of 50% of pure illite and 50% of pure smectite phases (detailed in Supplementary material, p. S5-S6). After drilling, the core samples were protected from oxygen with a container under $N_{2(g)}$. All manipulations were then carried out in a glovebox with $O_{2(g)}$ concentrations below 10 ppm. The rock cores were sliced using a wire saw, crushed with a mortar and entirely sieved under 125 µm. Before retention experiments, the rock powder was equilibrated during a week with a synthetic pore water, representative of *in situ* conditions, i.e. pH ~ 7.15, Ionic Strength (I.S.) ~ 0.1 M. The composition of synthetic pore water is detailed in supplementary data (Table S2). Some samples of COx clay rock were decarbonated. Two steps addition of diluted (0.1 M) and concentrated (1 M) HCl solutions was carried out for 8 hours with a maximum solid to liquid ratio m/V ~ 0.1 kg L^{-1}. The addition speed of the acid was adjusted to avoid pH below pH = 4 and potential damage to mineral surfaces. This step was followed by successive washings with Milli-Q® water (> 18 MΩ) and equilibration with 0.1 M NaCl solution. The level of dissolved carbonates released from decarbonated samples was quantified and found to be relatively low, i.e. total inorganic carbon: [T.I.C.] < 10^{-4} M released during batch experiments in absence of organic compounds (V/m > 10 L kg^{-1}).

The organic compounds studied are mainly small soluble organic acids. The list and chemical properties of the organic acids are given in supplementary information (Table S3). Organic sodium salts and acids with high purity (>99%) were purchased when commercially available. The synthesis of ISA isomers was performed based on the recipes of Whistler and BeMiller (1963) and Shaw (2013), as already reported in Dagnelie et al. (2014). Briefly, α-ISA was prepared by degradation of lactose in $Ca(OH)_2$. A mixture of α-ISA and β-ISA (noted β,α-ISA) was also obtained after purification of the precipitate obtained from cellulose degradation by pure slaked lime ($Ca(OH)_2$). The corresponding lixiviation colloidal suspension was kept and used as an analogue for β-ISA, α-ISA, x-ISA and other degradation side products (noted β,α,x-ISA). Organic solutions were prepared by dissolution in synthetic pore water. In the case of high concentration of oxalate and α-Isa, Milli-Q® water was used to avoid

precipitation of organic salts, e.g. $CaOx_{(s)}$, $Ca(Isa)_{2(s)}$. Before the sorption experiments, the pH of organic solutions was adjusted between 7 and 7.5 by addition of concentrated solutions of NaOH or HCl.

2.2. Adsorption experiments

Adsorption experiments were carried out at controlled room temperature, T = 21 ± 1°C and in anoxic glovebox ($N_{2(g)}$, $O_{2(g)}$ << 10 ppm) with controlled $p(CO_2)$ ~ 0.6 – 1%. Volume, mass and concentrations are detailed in supplementary information (Table S1). Briefly, a mass of solid, e.g. ~200 mg for U experiments, was mixed and equilibrated several days with synthetic pore water, eventually containing organic compounds. Solid to liquid ratios were typically in the range of m/V ~ 2.5×10^{-3} up to $1.25\ 10^{-2}$ g mL^{-1} for the europium experiments, and 5×10^{-2} up to 10^{-1} g mL^{-1} for the thorium and uranium experiments. The pH control for the uranium experiments was performed by adding aliquots of 0.1 M HCl solution, followed by 24h equilibration. Adsorption started with the addition of a small volume of synthetic solution containing the RN and eventual radioactive tracer in contact with the chosen mass of solid, i.e. dissolved Eu(III) / ^{152}Eu, Th(IV), ^{238}U(VI). The target concentrations were in the range $[Eu]_0$ ~ 10^{-9} M, $[Th]_0$ ~ $4\ 10^{-6}$ M, $[U]_0$ ~ 3×10^{-7} M. In the case of thorium, the initial concentration was above the observed solubility level in COx pore water observed without organic molecules, i.e. around $(4 \pm 3) \times 10^{-8}$ M controlled by equilibrium with respect to $ThO_{2(s)}$ (Rand et al., 2009). However, the strong sorption of thorium induced a decrease of $[Th]_{aq.}$ below solubility limit, within the first few hours, thus avoiding the precipitation of secondary solid phases. The system in batch was then mixed for 24 h to 14 days. For each sampling, the tubes were centrifuged at ~50,000 g for 1 hour. Small volumes of solution, 100 < dV < 250 µL, were collected for eventual dilution and measurement. The europium was measured using ^{152}Eu as a radiotracer and γ counting (Packard 1480 WIZARD 3). Thorium and uranium concentrations were quantified by mass spectrometry (ICP-MS 810-MS, AGILENT). To this aim, the samples were diluted in 2% HNO_3 solution with an addition of ^{208}Tl (~10^{-10} M) as an internal standard. The quantification limit (Q.L. = 3×σ) for uranium and thorium was found to be ~ 2×10^{-12} M and ~ 5×10^{-12} M respectively.

Sorption was quantified by a solid-solution distribution coefficient, noted R_d (L kg^{-1}) and defined by:

$$R_d = \frac{C_{ads}}{C_e} = \frac{n_0 - n_e}{m}\frac{V}{n_e} \quad (1)$$

where C_{ads} (mol kg^{-1}) is the concentration of sorbed species per mass of sorbent, C_e (mol L^{-1}) the concentration of the species in solution at equilibrium, n_0 (moles) and n_e (moles) the initial and equilibrium molar quantity in solution, V is the volume of solution, and m is the mass of dry solid sorbent. The method of error propagation, using partial derivate of Eq. (1) provided the uncertainty on R_d values, $\sigma(R_d)$, estimated with equation (2):

$$\sigma^2(R_d) = \left(\frac{1}{n_e}\frac{V}{m}\right)^2 \sigma^2(n_0) + \left(\frac{-n_0}{{n_e}^2}\frac{V}{m}\right)^2 \sigma^2(n_e) + \left(\frac{R_d}{m}\right)^2 \sigma^2(m) + \left(\frac{R_d}{V}\right)^2 \sigma^2(V) \quad (2)$$

2.3. Modelling

The modelling was performed with PHREEQC software (Phreeqc Interactive, Parkhurst and Appelo, 2013). The thermodynamic database "ThermoChimie" (Giffaut et al., 2014) was used to model speciation in solution (https://www.thermochimie-tdb.com). Concerning adsorption, several mechanistic models describe the sorption of RNs on clay minerals (Table 1). The description of solid solution interactions can be macroscopic (Reinoso-Maset and Ly, 2014) or microscopic (Bradbury and

Baeyens, 1997). Moreover, the model may use an electrostatic or non-electrostatic description of the system. Since 2000, important developments were specifically made on clayey minerals, e.g. multi-site ion exchange thermodynamic model (Motellier et al., 2003; Reinoso-Maset and Ly, 2014; 2016), or Two Site Protolysis Non-Electrostatic Surface Complexation and Cation Exchange model (2SPNE SC/CE, Bradubury et al., 2009a and 2009b). A simplified non-electrostatic surface complexation model was used in our study and described below.

Table 1. References describing mechanistic and empirical models developed on the sorption of RNs on clay minerals: surface complexation (SC), Two Site Protolysis Non-Electrostatic Surface Complexation and Cation Exchange (2SPNE SC/CE) and multi-site ion exchange model (MISE).

Reference	Model	Element	Material
Bradbury et al., 2005a Bradbury & Baeyens, 2009a&b Marques Fernandes et al., 2015 Gao et al., 2015 Maia, 2018	2SP-NE SC/CE	Eu, Cm, Ni, Co, Eu, Sn, Am, Th, Pa, U, Cs, Co, Ni, Eu, Th, U, U	Illite
Wissocq et al., 2018 Martin et al., 2018	MSIE	Cs, Sr, Tl	Illite & smectite
Pabalan and Turner, 1996 Bradbury & Baeyens, 2005b Tertre et al., 2009 Besançon et al., 2020 Marques Fernandes et al., 2012 Troyer et al., 2016 Tournassat et al., 2017	SC 2SP-NE SC/CE MSIE 2SP-NE SC/CE SC Spillover SC	U Mn, Co, Ni, Zn, Cd, Eu, Am, Sn, Th, Np, U Zn U, Ra U, U / phosphates U	Montmorillonite
Reinoso-Maset and Ly, 2014, 2016	MSIE	Ra, U	Kaolinite

The description of natural samples as an assemblage of pure phases, e.g. illite, smectite, iron (hydroxyl)oxides, is often used to predict cations adsorption (Joseph et al., 2013; Peynet, 2003). Yet, the prediction of distribution coefficients with high accuracies, i.e. $\sigma(\log_{10}R_d) < 0.3$, is not systematic on a wide range of conditions, i.e. pH, concentrations, speciation (Kautenburger et al., 2019; Marques Fernandes et al., 2015). For example, the competition sorption in presence of natural trace elements, e.g. Al^{3+}, Fe^{3+}, might bias some parameters of the model (Semenkova et al., 2018; Verma et al., 2019). As another example, experiments with U(VI) are sensitive to residual concentration of carbonates, e.g. $[T.I.C.] < 5 \times 10^{-5}$ M, which may also bias experimental data and interpretation of results (Tournassat et al., 2017). The focus of this study being the effect of organic plume on the retention of RNs, we tried to firstly assess the possible sources of bias due to model hypotheses. A one-site simplified sorption model, with a mass fraction of "pure" illite, was then considered as the sorbing phase. The Surface complexation constants used in this study are provided in Table 2. Only the strong sorption site was considered, given the low contribution of weak sites (Descostes et al., 2017) under the experimental concentration ranges. Considering the relatively high ionic strength (IS) in COx pore water, IS(COx) ~ 0.1 M, the contribution of cation exchange was also neglected (Bradbury and Baeyens, 2002; Tournassat et al., 2013). Available surface complexation constants were assessed using sorption data in the absence of organic molecules and gathered in Table 2.

Table 2. Surface complexation model of binary systems: RN / COx. Data on strong sites from references: Bradbury et al., 2005a [a], 2005b [b], 2005c [c], 2009a [d], 2009b [e], 2011 [f]; Jospeh et al. 2013 [g], Maia, 2018 [h], Marques-Fernandes et al., 2015 [i]. *Adjusted in this work.

Sorbate	Surface complexation equation	$log_{10}K°$ (this study)	$log_{10}K°$ Illite	$log_{10}K°$ Montmorillonite
	Strong site concentration (moles kg^{-1}) →	2×10^{-3}	2×10^{-3} [a,b,c]	2×10^{-3} [d,e]
Proton	$Clay\_sOH + H^+ = Clay\_sOH_2^+$	4.9	4.0[d,h], 4.9[g], 5.5[b]	4.5[h]
	$Clay\_sOH = Clay\_sO^- + H^+$	-6.8	-6.2[d,h], -6.8[g]	-7.9[h]
Am(III)	$Clay\_sOH + Am^{3+} = Clay\_sOAm^{2+} + H^+$	3.1	3.1[a], 3.1[e]	0.5[a]
	$Clay\_sOH + Am^{3+} + H_2O = Clay\_sOAm(OH)^+ + 2H^+$	-4.5	-3.9[a], -4.5[e]	-5.6[a]
	$Clay\_sOH + Am^{3+} + 2\ H_2O = Clay\_sOAm(OH)_2 + 3H^+$	-13.0	-13.3[a], -13.0[e]	-14.8[a]
	$Clay\_sOH + Am^{3+} + 2\ H_2O = Clay\_sOAm(OH)_3^- + 4H^+$	-24.3	-24.3[e]	
Eu(III)	$Clay\_sOH + Eu^{3+} = Clay\_sOEu^{2+} + H^+$	3.1	3.1[a,c], 1.9[e,f]	0.6[a], 1.9[f]
	$Clay\_sOH + Eu^{3+} + H_2O = Clay\_sOEuOH^+ + 2H^+$	-4.4	-4.4[a,c], -4.6[e,f]	-6.2[a], -6.4[f]
	$Clay\_sOH + Eu^{3+} + 2\ H_2O = Clay\_sOEu(OH)_2 + 3H^+$	-12.7	-12.7[a,c], -12.8[e,f]	-14.2[a], -15.7[f]
	$Clay\_sOH + Eu^{3+} + 2\ H_2O = Clay\_sOEu(OH)_3^- + 4H^+$	-24	-24[e,f]	
Th(IV)	$Clay\_sOH + Th^{4+} = Clay\_sOTh^{3+} + H^+$	7.4	7.4[d,e]	7.2[b,f]
	$Clay\_sOH + Th^{4+} + H_2O = Clay\_sOTh(OH)^{2+} + 2\ H^+$	2.3	2.3[d,e]	2.7[b,f]
	$Clay\_sOH + Th^{4+} + 2\ H_2O = Clay\_sOTh(OH)_2^+ + 3\ H^+$	-2.4	-2.4[d,e]	-2.6[b,f]
	$Clay\_sOH + Th^{4+} + 3\ H_2O = Clay\_sOTh(OH)_3 + 4\ H^+$	-8.8	-8.8[d]	-9.1[b,f]
	$Clay\_sOH + Th^{4+} + 4\ H_2O = Clay\_sOTh(OH)_4^- + 5\ H^+$	-15.3	-15.3[d,e]	-16.9[b,f]
U(VI)	$Clay\_sOH + UO_2^{2+} = Clay\_sOUO_2^+ + H^+$	2.0	2.0[b,g], 2.0[e,h], 2.6[c]	
	$Clay\_sOH + H_2O + UO_2^{+2} = Clay\_sOUO_2(OH) + 2\ H^+$	-4.2	-4.2[b,g], -3.5[e,h], -3.6[c]	
	$Clay\_sOH + 2\ H_2O + UO_2^{2+} = Clay\_sOUO_2(OH)_2^- + 3\ H^+$	-10.9	-10.9[b,g], -10.6[e,h], -10.3[c]	
	$Clay\_sOH + 3\ H_2O + UO_2^{2+} = Clay\_sOUO_2(OH)_3^{2-} + 4\ H^+$	-18.21	-18.21[b,g], -19[e,h], -17.5[c]	
	$Clay\_sOH + UO_2^{2+} + CO_3^{2-} = Clay\_sOUO_2(CO_3)^- + H^+$	11.2*		9.8[i,h]
	$Clay\_sOH + UO_2^{2+} + 2\ CO_3^{2-} = Clay\_sOUO_2(CO_3)_2^{3-} + H^+$	or 16.95*	17.5[h]	15.5[i], 15[h]

Eventual differences are rather small and do not affect further discussion. The initial concentration of RNs in speciation calculations were taken equal to experimental values, e.g. $[Eu]_0 \sim 10^{-8}$ mol L^{-1}. Corresponding data are detailed in Table S1. The initial composition of solution in the model was based on theoretical pore water composition (Table S2), with addition of variable amounts of organic compounds under sodic form, e.g. Na_2(o-phthalate) from 10^{-9} to 1 mol L^{-1}. Equilibrium with calcite ($CaCO_{3(s)}$) was imposed in the model. Solution to solid ratios, V/m, were taken equal to experimental values (Table S1) and corresponding site density and calcite content reprocessed for 1 kg of solution in PhreeqC scripts. Since no sorption of organic molecules was assumed in the model, the concentration of organic compounds from the model was directly compared to the experimental value at equilibrium. Concentration of organic compounds at equilibrium, C_e(Organic), was not easily measurable because of the presence of dissolved natural organic matter (Glaus et al., 2005; Grasset et al., 2010; Huclier-Markai et al., 2010). C_e(Organic) was then calculated from the initial concentration, C_0(Organic). To that aim, the sorption of organic compounds on COx clay rock (Rasamimanana et al., 2017) was described by Langmuir Equation:

$$R_d = \frac{K \times Q}{1 + K \times C_e} \quad (3)$$

where K (L mol^{-1}) is an affinity constant and Q (mol kg^{-1}) a maximum sorbed amount. The expression of R_d(Organic) = f(C_0, C_e) from Eq. (1) can be replaced in Eq. (3) and the isolation of C_e(Organic) as a function of other parameters leads to the following equation:

$$C_e = \frac{-(1 + KQm/V - KC_0) + \sqrt{(1 + KQm/V - KC_0)^2 + 4KC_0}}{2K} \quad (4)$$

The Langmuir sorption parameters used to calculate C_e(Organic), i.e. K(Organic/COx) and Q(Organic/COx), are taken from Rasamimanana et al. (2017) and gathered in Table S4.

3. Results

3.1. Adsorption of Eu(III) on COx clay rock

In the absence of RNs, organic compounds form complexes with cations present in COx pore water (Dagnelie et al., 2014). The corresponding speciation is provided in Table S4. Note that the solubilities of oxalate and α-ISA in COx pore water are relatively low: $s(Ca(Ox)_{(s)}/COx) \sim 2 \times 10^{-5}$ M and $s(Ca(\alpha\text{-}Isa)_{2(s)}/COx) \sim 7 \times 10^{-3}$ M, respectively. Fig. 1a shows europium sorption on COx clay rock as a function of concentration of organic compounds. Values at 10^{-9} M correspond to sorption experiments without addition of organic compound, i.e. with only D.O.M.. Complementary speciation data in solution are detailed in supplementary data (Fig. S1). The sorption isotherms display a plateau at low organic concentrations followed by a decrease due to the complexation above a so-called "concentration edge" (Tits et al., 2005; Guo et al., 2015). The concentration edges are representative of the strength of the complexation of Eu(III) by the organic compounds, i.e. $\log_{10}\beta°$(Eu-Organic) versus $\log_{10}\beta°$(Ca/Mg-Organic). The selectivity of organic compounds inducing a decrease of Eu(III) retention follows the order: EDTA > tartrate ~ citrate > α-ISA > o-phthalate, with corresponding concentration edges: 0.5-2 $\times 10^{-7}$ M, 1-2 $\times 10^{-5}$ M, 2 $\times 10^{-4}$ M, 0.3-1 $\times 10^{-2}$ M. In the case of multidentate species, such as EDTA, a secondary phenomenon may occur, which is the sorption of the [RN-Organic] complex. In this case, a second plateau appears, as observed when [EDTA] > 2 $\times 10^{-3}$ M (Fig. 1a). Such specific behaviour was reported in Descostes et al. (2017), with similar behaviours quantified for Eu-$EDTA^-$ and Ca-$EDTA^{2-}$.

On a log-log plot (Fig. 1a), the slope of the sorption edges indicates the stoichiometry of the RN / Organic complexation reaction. EDTA, o-phthalate and α-ISA form 1:1 complexes with Eu(III), leading to a decrease of R_d(Eu(III)) with a slope (-1). In the case of citrate, two organic molecules form $[Eu(Cit.)_2]^{3-}$ complexes, as shown by speciation calculation (Figure 1b). The stoichiometry 1:2 of the formed complexes induces a decrease of R_d(Eu(III)) with a slope (-2), as illustrated in Figure 1a. In the case of o-phthalate, the formation of mono- and di-phthalate complexes is also included in *ThermoChimie* TDB (Table 3): $\log_{10}\beta°_1(Eu(o\text{-phthalate}))^+ = 4.96$ and $\log_{10}\beta°_2(Eu(o\text{-phthalate})_2)^- = 7.34$. The experimental isotherm displays a shape analogue to the predictive model. The small gap between the phthalate experimental and modelled curves is not significant, regarding the variability of the value of the plateau in absence of organic compounds. Such variability is illustrated in Fig. 1, with the dashed line corresponding to the model for phthalate, assuming a quantity of sorption site doubled.

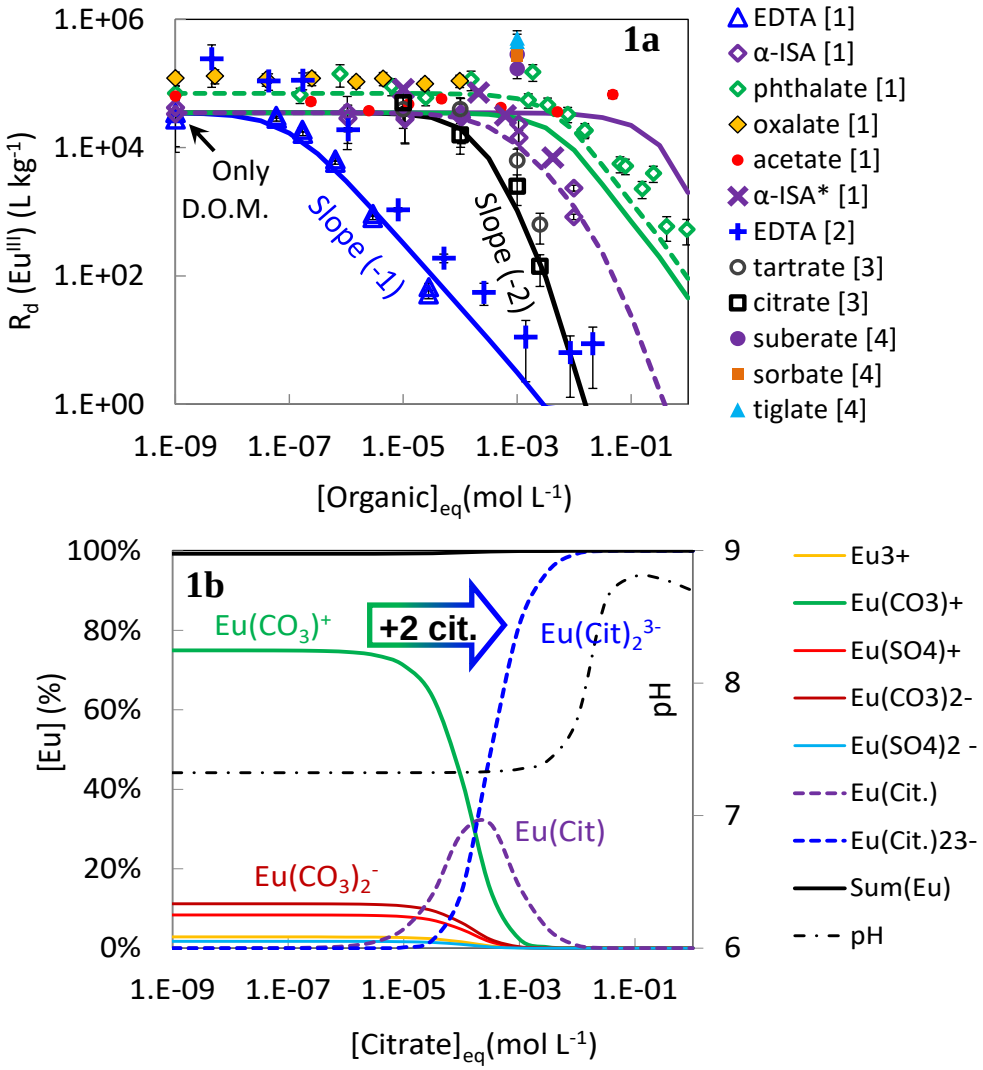

Fig. 1. Adsorption of Eu(III) on COx clay rock as a function of concentration of various organic compounds. (1a) Experimental data compared with surface complexation predictive model using *ThermoChimie* TDB (solid lines). Dashed lines correspond to adjusted model (this work). (1b) Speciation of europium in COx pore water as a function of citrate concentration. $[Eu]_0$ ~ 1-2 10^{-8} M (detailed in Table S1). [1] This study. [2] Descostes et al. 2017, [3] Schott et al., 2012 on Opalinus clay [4] Vu-do 2013. *(ISA mixed with other organic compounds).

Table 3. Main data used for complexation between organic compounds and radionuclides (Exhaustive dataset in Table S5). Complexation constants, log10K° (25°C, I.S. = 0). Values in italic reprocessed at I.S. = 0 using Davies equation. TDB : "ThermoChimie" Database V10a (https://www.thermochimie-tdb.com/). *Value with hypothesis $\nu_i(H^+) = +4$ not recommended. $^{\$}$Reviewed in Tits et al. 2005)

RN	Ligand	$\log_{10}K°$ (I.S. = 0)	Reference	Reaction
Eu(III)	EDTA	19.67	This work (analogy with Am)	$Eu^{3+} + Edta^{4-} = Eu(Edta)^-$
	Citrate	8.55	This work (analogy Am)	$Eu^{3+} + Cit.^{3-} = Eu(Cit)_{(aq.)}$
		13.9		$Eu^{3+} + 2\ Cit.^{3-} = Eu(Cit)_2^{3-}$
	α-ISA	-20.9	TDB	$Eu^{3+} + H_4ISA^- + (3\text{-}x)\ H_2O = Eu(OH)_{3-x}(H_{4-x}ISA)^- + 3H^+$
		-16.3 ± 0.3	This work (pH ~ 7.2)	
		-18.2	Van Loon et al., 1998	
		-19.2	Vercammen et al., 2001$^{\$}$	
		-20.9	Tits et al., 2005 (pH ~ 13.3)	
		-18.5		$Eu^{3+} + H_5GLU^- = Eu(H_2GLU)^- + 3H^+$
		*-30.6**	Vercammen et al., 2001*	$Eu^{3+} + H_4ISA^- + (4\text{-}x)\ H_2O = Eu(OH)_{4-x}(H_{4-x}ISA)^{2-} + 4H^+$
		-31.1	Tits et al., 2002	
	o-phthalate	4.96	TDB	$Eu^{3+} + Phthal^{2-} = Eu(Phthal)^+$
		7.34	TDB	$Eu^{3+} + 2\ Phthal^{2-} = Eu(Phthal)_2^-$
Th(IV)	α-ISA.	-5.65	TDB	$Th^{4+} + H_4ISA^- + 3\ H_2O = Th(OH)_3(H_4ISA) + 3H^+$
		-13.2	TDB	$Th^{4+} + H_4ISA^- + 4\ H_2O = Th(OH)_4(H_4ISA)^- + 4H^+$
		-9	TDB (analogy with gluconate)	$Th^{4+} + Ca^{2+} + H_4ISA^- + 4\ H_2O = CaTh(OH)_4(H_4ISA)^+ + 4H^+$
		-10 ± 0.3	This work	
		-10.1	Hummel et al., 2005	$Th^{4+} + H_4ISA^- = Th(H_4ISA)^{3+}$
		-5.0	Hummel et al., 2005	$Th^{4+} + Ca^{2+} + 2\ H_4ISA^- = CaTh(H_2ISA)_2 + 4H^+$
	Citrate	16.8*	TDB*	$Th^{4+} + Cit^{3-} = Th(Cit)^+$
		13.7	Hummel et al., 2005	
		25.8*	TDB*	$Th^{4+} + 2\ Cit^{3-} = Th(Cit)_2^{2-}$
U(VI)	Ca^{2+} CO_3^{2-}	27.2	Shang and Reiller, 2020	$Ca^{2+} + UO_2^{2+} + 3\ CO_3^{2-} = CaUO_2(CO_3)_3^{2-}$
		27.18	TDB	
		27.0 ± 0.2	Grenthe et al., 2020	
		30.49	Shang and Reiller, 2020	$2\ Ca^{2+} + UO_2^{2+} + 3\ CO_3^{2-} = Ca_2UO_2(CO_3)_3$
		30.7	TDB	
		30.8 ± 0.4	Grenthe et al., 2020	
	Citrate	8.96	TDB	$UO_2^{2+} + Cit^{3-} = UO_2(Cit)^-$
	α-ISA	3.70	TDB	$UO_2^{2+} + H_4ISA^- = UO_2(H_4ISA)^+$
		6.60	TDB	$UO_2^{2+} + 2\ H_4ISA^- = UO_2(H_4ISA)_2$
	o-phthalate	5.56	TDB	$UO_2^{2+} + Phthal^{2-} = UO_2(Phthal)$
	Succinate	5.28	TDB	$UO_2^{2+} + Succin^{2-} = UO_2(Succin)$

One main discrepancy between experimental and modelled data appears in presence of α-ISA. The ISA isomers are major degradation products of cellulose (Glaus et al., 1999; Van Loon et al. 1999, Rout et al., 2015, Shaw 2013). Most of the complexation data on α-ISA and analogues, such as gluconate (Dudás et al., 2017), have been measured at high pH, e.g. pH = 13.3 in Tits et al. (2005). It is assumed that the complexation mechanism between trivalent actinides and α-ISA includes a release of 3 or 4

protons at high pH , for example leading to Eu(HISA) as considered in Vercammen et al. (2001) or Tits et al. (2005). Such complexation reaction may involve either the deprotonation of isosaccharinate or the deprotonation of water molecules. Thus, in the absence of spectroscopic evidences on the structures of these complexes, the general formalism from equation (5) is recommended (Hummel et al., 2005):

$$Eu^{3+} + H_4ISA^- + (3-x)\,H_2O = Eu(OH)_{3-x}(H_{4-x}ISA)^- + 3H^+ \quad (5)$$

It is to note that a single constant, $\log_{10}K°$(Eq. 5), can be considered, independently of the "real" value of x. Several values of $\log_{10}K°$(Eq. 5) were quantified at high pH (Table 3), ranging from -18.2 (Van Loon and Glaus, 1998, pH > 10), down to -20.9 (Tits et al., 2005, pH = 13.3), this latter value and a stoichiometric coefficient x = 0 being considered in *ThermoChimie* TDB. However, none of these values could predict correctly the experimental results on COx clay rock (pH ~ 7.2). A value of $\log_{10}K°$(Eq.5) = -16.3 ± 0.3 was then adjusted by fitting our experimental data (Fig. 1a, dashed lines). Although, the data on Eu(III) may display uncertainties due to the hydrolysis constants on Eu(III) (Hummel et al., 2005; Tits et al., 2005) the significant difference, i.e. 2 to 4 orders of magnitude, between our complexation constant (-16.3 at neutral pH) and other data (-18.2 down to -20.9 at pH=13.3) seems unlikely for a similar reaction. Such discrepancy may suggest that the underlying mechanisms differ and that two different reactions are occurring at pH 7.2 and pH 13.3. Taking this into consideration, the reaction may be more appropriately represented by Eq. 6:

$$Eu^{3+} + H_4ISA^- + (n-x)\,H_2O = Eu(OH)_{n-x}(H_{4-x}ISA)^{2-n} + nH^+ \quad (6)$$

Hence, one possible explanation of the differences observed according to pH would be that n value is lower at neutral pH (e.g. n = 2 in COx, with a neutral $Eu(OH)_{2-x}(H_{4-x}ISA)^0$ complex, table S5), than at high pH (n = 3 or 4 above pH > 10, with anionic species such as $Eu(OH)_{3-x}(H_{4-x}ISA)^-$). This result encourages for further investigation, as performed for other systems such as Pu(III) (Tasi et al., 2018), in order to determine the structures of Eu(III)-ISA predominant species as a function of pH, the values of n and x, and corresponding complexation constants.

3.2. Adsorption of Th(IV) on COx clay rock

The sorption of Thorium on COx clay rock displays similar results to Eu(III) (Figure 2a). Experimental data for Th(IV) are given for the highly complexing species: citrate, α-ISA, o-phthalate. Some sorption edges of Th(IV) isotherms appear for [Cit.] > 10^{-4} M and [α-ISA] > 5×10^{-4} M. A relatively good agreement is observed between experimental data and predictive modelling. This result confirms both the relevancy of the simplified sorption model and the accuracy of TDB to calculate speciation.

In the case of α-ISA, the concentration edge and slope of the sorption isotherm, (-1), were correctly predicted by the model. The corresponding complexes from "ThermoChimie" thermodynamic database are $Th(OH)_{4-x}(H_4ISA_{-xH})^-$ and $CaTh(OH)_{4-2y}(H_4ISA_{-yH})^+_{(aq)}$, with the values of x being unknown. For this latter complex, the value of $\log_{10}\beta°$ $(CaTh(OH)_4(Glu)^+) = -9$ is defined by analogy with gluconate (Colàs et al., 2013). A similar value can be adjusted with our results, i.e. $\log_{10}\beta°$ $(CaTh(OH)_{4-2y}(H_4ISA_{-yH})^+) = -10.0 \pm 0.3$ (Table 3), as illustrated in Fig. 2. In contrast to trivalent actinides, Th(IV) data shows a good agreement between complexation constants at high pH (Vercammen et al., 2001; Colàs et al., 2013) and neutral pH (this study). This likely indicates a similar reaction of Th(IV) with α-ISA at both pH. This assumption is corroborated by the speciation of Th(IV),

which is driven by hydroxides of thorium, even at neutral pH (Fig. S2b), whereas speciation of Eu(III) is dominated by Eu-CO_3^+ and Eu$(SO_4)^-$ complexes at neutral pH. Lastly, at higher concentrations, [α-ISA] > 2×10^{-2} M, an increase of R_d(Th(IV)) is observed. This retention is probably due to the precipitation of Th-ISA complexes, or more likely the co-precipitation with $Ca(H_4(\alpha\text{-ISA}))_{2(s)}$. The absence of significant complexation between o-phthalate and Th(IV) is confirmed by modelling.

The main discrepancy between Th(IV) experimental and modelled data appears in the presence of citrate. The concentration edge of the sorption isotherm, above [citrate] > 5×10^{-5} M, fits well with the model. However, a slope (-2) is expected from the model, versus (-1) measured experimentally. Reactions between Th(IV) and citrate have been well studied (Choppin et al., 1996; Felmy et al., 2006) and corresponding constants have been quantified with accuracy (Hummel et al., 2005). The formation of $(Th(Cit.)_2)^{2-}$ is then expected above 10^{-4} mol L^{-1} of citrate, as shown in Fig. 2b in speciation calculation. Yet, the experimental slope (-1) indicates a stoichiometry 1:1 between the Th(IV) sorbed species and predominant species in solution $(Th(Cit.)_2)^{2-}$. A possible explanation is that $(Th(Cit.))^+$ may sorb on COx clay rock, with values 0 << $R_d(Th(Cit.)^+/COx)$ << R_d(Th(IV)/COx). This hypothesis would explain the decrease of R_d(Th) with a slope (-2) until its value becomes close to $R_d(Th(Cit.))^+$. Then the complexation of $Th(Cit)^+$ by additional citrate, with a stoichiometry 1:1, would explains the decrease with a slope (-1), as observed at higher concentrations of citrate. This hypothesis is in agreement with sorption values previously measured for citrate on COx clay rock: R_d(Citrate / COx) ~ 30-60 L kg^{-1} (Rasamimanana et al., 2017), as well as multidentate complexes, e.g. Eu-$EDTA^-$ in the case of europium (Descostes et al., 2017). Thus, further investigations, such as *in-situ* spectroscopic studies, would be interesting to confirm thorium retention mechanism in presence of high citrate concentration.

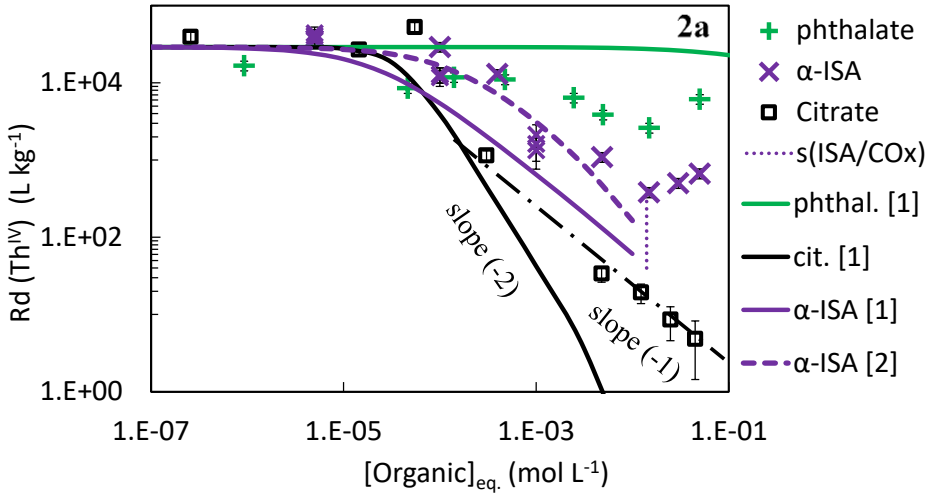

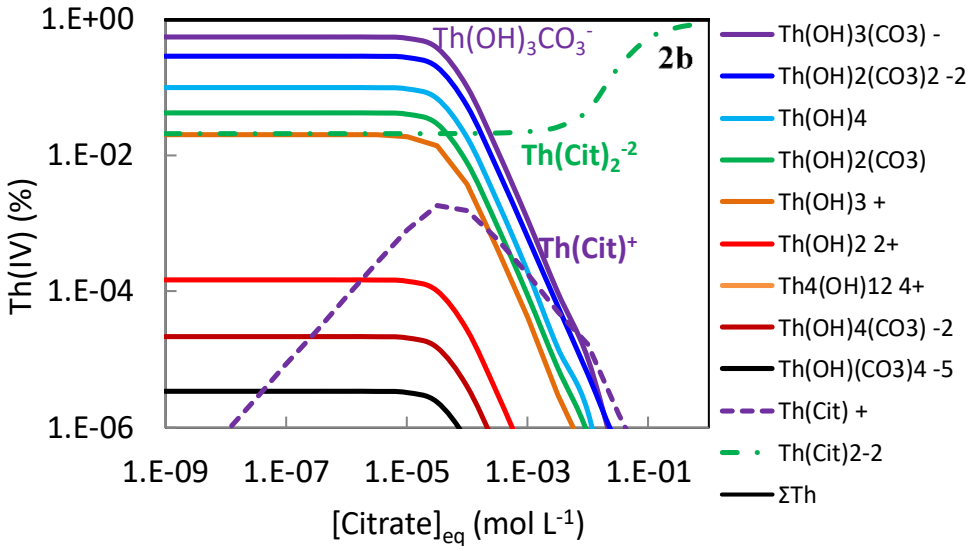

Fig. 2. Adsorption of Th(IV) on COx clay rock as a function of concentration of various organic compounds. (2a) Experimental data compared with surface complexation predictive model using *ThermoChimie* TDB (solid lines) [1]. $[Th]_0 \sim 4\ 10^{-6}$ mol L^{-1}, V/m ~ 20 L kg^{-1}, pH ~ 7.2 (detailed in Table S1). s(ISA) = solubility of $Ca(HISA)_{2(s)}$ in COx pore water. [2] (Dashed line) Model with adjusted value $\log_{10}\beta°(CaTh(OH)_4(H_4ISA)^+)$. (2b) Speciation of thorium in COx pore water as a function of citrate concentration.

3.3. Adsorption of U(VI) on COx clay rock

The predictive modelling of U(VI) sorption on COx clay rock can be derived from several models developed on pure clay minerals (Pabalan and Turner, 1996; Bradbury and Baeyens, 2005b, 2009b; Marques Fernandes et al., 2012; Reinoso-Maset et al., 2014). When applied on natural samples, accuracy may be affected by the hypotheses on sorbing phases (Joseph et al. 2013), sorption mechanisms (Marques Fernandes et al., 2015; Maia 2018), or surface complexation constants (Tournassat et al., 2017). Figure 3 compares the experimental data with some surface complexation models available in the literature. The solid-solution distribution ratio measured in absence of organic compounds is $R_d(U(VI)/COx) = 7.5$ L kg^{-1} with a variability $\sigma = 1.6$ L kg^{-1}. All models predict a low retention of U(VI) in comparison with other RNs, i.e. $R_d(U(VI)/COx) << 10^2$ L kg^{-1}, due to the formation of ternary species $Ca_xUO_2(CO_3)_y^{2(y-1-x)-}$ (Bernhard et al., 2001; Shang and Reiller, 2020). Yet, some significant discrepancies subsist between models. Before assessing the disturbance by organic compounds, the following section details the choice and adjustment made in this work on sorption model for U(VI).

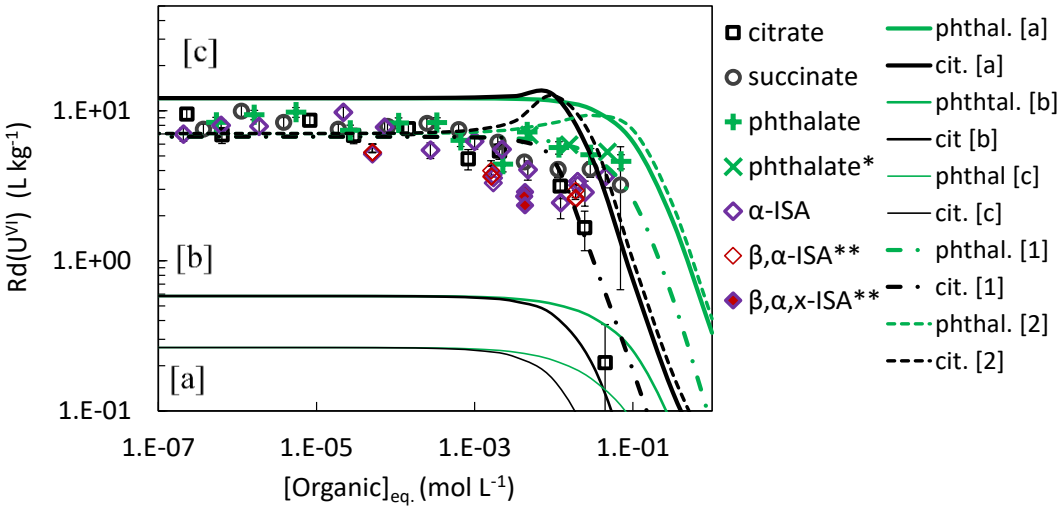

Fig. 3. Adsorption of U(VI) on COx clay rock as a function of concentration of various organic compounds at equilibrium with calcite. $[U]_0$ ~ 5 10^{-7} mol L^{-1}, V/m ~ 10 L kg^{-1}, pH ~ 7.2 (detailed in Table S1). Signs: experimental results. Solid lines: predictive modelling based on data from, Bradbury & Baeyens, 2009b[a], Joseph et al., 2013[b], Maia, 2018[c]. Dashed lines: adjusted model with $\log_{10}K_1°(\text{Clay\_sOUO}_2(\text{CO}_3)^-)$[1] or $\log_{10}K_2°(\text{Clay\_sOUO}_2(\text{CO}_3)_2^{3-})$[2] as parameter. *Organic compounds within mixtures (Table S1).

3.3.1. Modelling adsorption of U(VI) in absence of organic compounds

Several parameters of the model affect significantly the value R_d(U(VI)/COx): Uranyl complexation in solution, i.e. $\log_{10}\beta°(\text{CaUO}_2(\text{CO}_3)_3^{2-})$, $\log_{10}\beta°(\text{Ca}_2\text{UO}_2(\text{CO}_3)_3)$ (Table 3); and sorption site properties, mostly $\log_{10}K°(\text{Clay\_sOH}_2^+)$, $\log_{10}K°(\text{Clay\_sOUO}_2^+)$, $\log_{10}K°(\text{Clay\_ sOUO}_2(\text{CO}_3)^-)$ and $\log_{10}K°(\text{Clay\_ sOUO}_2(\text{CO}_3)_2^{3-})$ (Table 2).

The complexation constants of U(VI) by calcium and carbonates in solution has been largely investigated (Dong and Brooks, 2006; Kalmykov and Choppin, 2009). Some recent studies provide dependency of complexation constant with temperature (Maia, 2018) and effect of ionic strength (Shang and Reiller, 2020). In this latter work, the constants $\log_{10}\beta°(\text{CaUO}_2(\text{CO}_3)_3^{2-})$ = 27.2 ± 0.04 and $\log_{10}\beta°(\text{Ca}_2\text{UO}_2(\text{CO}_3)_3)$ = 30.49 ± 0.05 are estimated accurately at infinite dilution, in agreement with data from Dong and Brooks (2006) used in *Thermochimie* TDB (Table 2). In addition, Shang and Reiller (2020) quantified the coefficients to account for specific ion interactions at high ionic strength (SIT): $\varepsilon(\text{CaUO}_2(\text{CO}_3)_3^{2-}, \text{Na}^+)$ = (0.29 ± 0.11) and $\varepsilon(\text{Ca}_2\text{UO}_2(\text{CO}_3)_{3(aq)}, \text{NaCl})$ = (0.66 ± 0.12) kgw mol^{-1}. For this reason, the data from Shang and Reiller (2020) was used in the model, in order to include SIT coefficients. The corresponding data on $\text{Mg}_x\text{UO}_2(\text{CO}_3)_3^{2(x-2)}{}_{(aq)}$ are also missing from *Thermochimie* TDB. This does not affect the following work, especially given the lower complexation constants between $(\text{UO}_2(\text{CO}_3)_3)^{4-}$ with Mg^{2+}, as compared to Ca^{2+} (Table S5).

Concerning the acidity of sorption strong site, $\log_{10}K°(\text{Clay\_sOH}_2^+)$, the reported data for illite varies between 4.0 and 5.5 (Table 2). It is to note that this value strongly affects the model parameters, eventually accounting for differences between published data set. However, the choice of the value 4.9 in this work is confirmed and forced by experimental data on Eu(III), as previously discussed.

The major uncertainties on U(VI) sorption modelling comes from the constants of surface complexation. Major discrepancies exist between studies, especially due to model hypotheses or experimental bias (Tournassat et al., 2017). For example, the consideration of uranyl-carbonate surface complexes, varies between studies (Table 2). The models on U(VI) / illite system derived from Joseph et al. (2013) and Bradbury and Baeyens (2009b) underestimate experimental values of R_d(U(VI)/COx) by an order of magnitude (Fig. 3). However, these models do not consider sorption of uranyl-carbonate surface complexes, despite evidences on montmorillonite (Marques Fernandes et al., 2012) or γ-alumina (Jo et al., 2018). Recently, Maia (2018) interpreted experimental data on COx clay rock, by considering the possible sorption of $UO_2(CO_3)_x^{2(1-x)}$ species. This model fits rather well the experimental data in absence of organic compounds (Fig. 3). However, we could not use directly these parameters, since the authors adjusted their dataset with values $\log_{10}K°(Clay\_sOH_2^+)$ = 4.0 (table 2) and $\log_{10}\beta°(CaUO_2(CO_3)_3^{2-})$ = 29.7 (Table 3), significantly differing from the values chosen in present work. We then had to adjust one surface complexation constant in order to reproduce the value of the plateau, R_d(U(VI)/COx) = 7.5 ± 1.6 L kg^{-1} below $[organic]_{eq.} < 10^{-3}$ M. The best-fit modelling are illustrated in Fig. 3 and the corresponding parameters are $\log_{10}K_1°(Clay\_sOUO_2(CO_3)^-)$ = 11.15 ± 0.1 or $\log_{10}K_2°(Clay\_sOUO_2(CO_3)_2^{3-})$ = 16.95 ± 0.1 (Table 2). Both values are in the range of parameters adjusted by Marques Fernandes et al. (2012) on montmorillonite and Maia (2018) on COx clay rock. However, such agreement does not provide any evidence for the existence of one or the other of these uranyl-carbonate surface complexes. This hypothesis is still a matter of debate (Tournassat et al., 2017), and is discussed furtherly with regard to effect of organic compounds.

3.3.2. Adsorption of U(VI) in presence of organic compounds

In presence of organic compounds, several phenomena occur simultaneously and may affect sorption, e.g. uranyl complexation, modification of aqueous speciation, phase dissolution, pH drift. Figure 4a illustrates Ca speciation in COx pore water, as a function of citrate concentration. Ca^{2+} is the predominant calcium species in absence of citrate. The complex $(Ca(Cit))^-$ becomes predominant above $[Cit]_{eq.} \sim 10^{-2}$ mol L^{-1} and Ca^{2+} becomes less available.

Fig. 4b shows the corresponding effect on U(VI) speciation. The $Ca_2UO_2(CO_3)_3$ and $CaUO_2(CO_3)_3^{2-}$complexes are the predominant species in raw COx pore water. This speciation explains the high sensitivity of the model to the surface complexation constants, $K_1°$ and $K_2°$, discussed previously. The addition of citrate induces two successive mechanisms. Firstly the depletion of free Ca^{2+}, above $[Cit]_{eq.} \sim 10^{-2}$ mol L^{-1}, causes the shift of U(VI)/Ca/CO_3 speciation, from $Ca_2UO_2(CO_3)_3$ to $CaUO_2(CO_3)_3^{2-}$. Then, only at high concentrations, $[Cit]_{eq.} > 10^{-1}$ mol L^{-1}, $UO_2(Cit)^-$ becomes predominant.

Regarding the effect of organic compounds on uranium sorption, a systematic decrease of R_d(U(VI)/COx) is quantified above 10^{-3} M in organic compounds (Fig. 3), seemingly similar to Eu(III) and Th(IV) cases. However, two striking specificities appear for uranium, as compared to other RNs. Firstly, the organic concentration edge is barely depending on the type of organic compounds (Fig. 3), i.e. the decrease of R_d(U(VI)/COx) starts at similar concentrations independently of the type or organic compound. Secondly, the decrease of R_d(U(VI)/COx) appears before the formation of uranyl-organic complexes (Fig. 4). These observations underline a different mechanism discussed below. As many natural media, COx clay rock displays carbonate minerals, e.g. calcite ($CaCO_{3(s)}$), dolomite ($MgCa(CO_3)_{2(s)}$), siderite ($FeCO_{3(s)}$). These minerals provide an important stock of soluble carbonates and calcium, potentially buffering the disturbance caused by organic plume (Geoffroy et al., 1999). In presence of carboxylic acids such as citrate, the dissolution of carbonate phases induces an increase of aqueous carbonates, CO_3^{2-}, leading to both an increase of [T.I.C.], and a drift in pH (Fig. 4a).

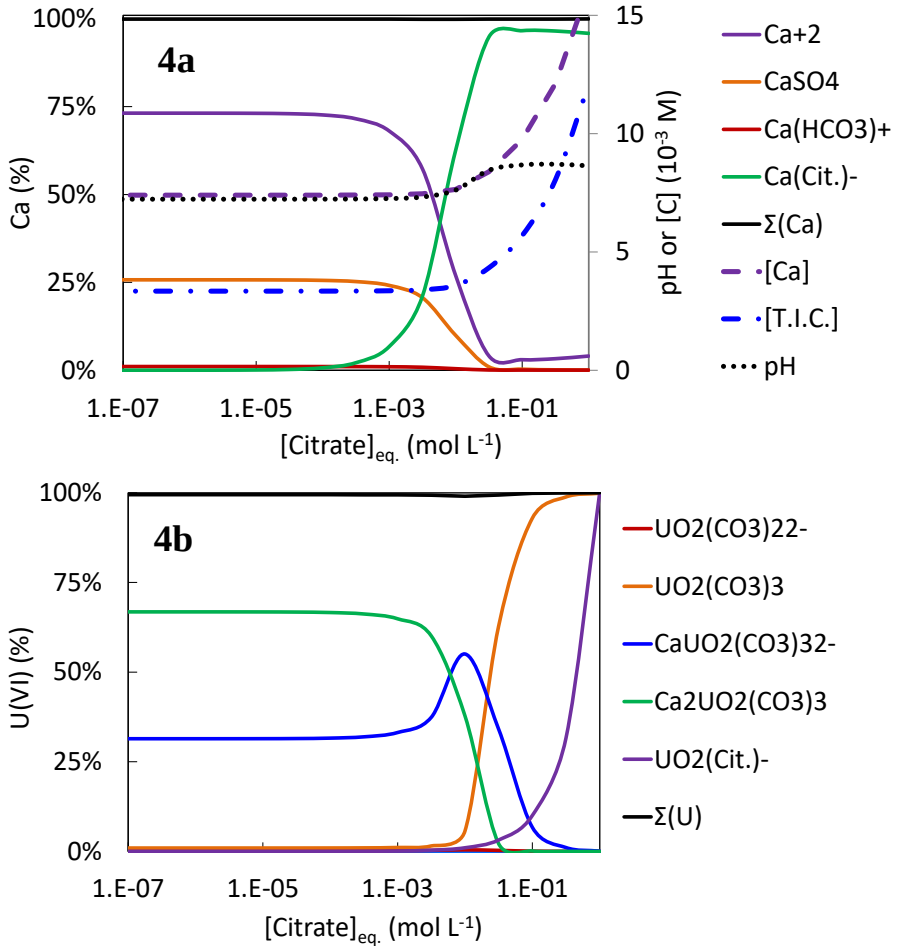

Fig. 4. Speciation of calcium (4a) and U(VI) (4b) in COx pore water as a function of citrate concentration with equilibrium with calcite in COx clay rock. $[U(VI)]_{eq.} = 3 \times 10^{-7}$ mol L^{-1}.

This dissolution also induces a release of calcium in solution, up to $[Ca]_{eq.} \sim 15\ 10^{-3}$ mol L^{-1} for $[Cit]_{eq.} \sim 1$ mol L^{-1}. Below [Cit.] = 10^{-1} mol L^{-1}, the sorption of uranyl is not affected by a direct complexation, as the complex U(VI)-citrate is barely formed. More likely, the disturbance of pore water chemistry, i.e. the increase of $[Ca^{2+}]_{eq.}$ and $[CO_3^{2-}]_{eq.}$, induces an additional complexation of uranyl compared to undisturbed COx pore water, and the following decrease of the value R_d(U(VI)/COx).

In order to quantify such disturbance, we measured the composition of pore water in presence of high concentrations of citrate and α-ISA. Fig. 5 shows the corresponding evolution of pore water chemistry. The experimental data highlights a disturbance of the system in two "steps". A first stock of cations, acting as a buffer, comes from the clay mineral surfaces. During the first step, the sorbed cations are leached from surfaces, as quantified by the increase of [Ca] and [Mg], without main modification of [T.I.C.]. Then, at higher concentrations, carbonate phases act like a second buffer. The dissolution of carbonates leads then to a simultaneous increase of both [Ca+Mg] and [T.I.C.] and a decrease of uranyl sorption. This "desorption" phenomenon is then indirectly due to the dissolution of carbonate minerals by carboxylates, more than a direct complexation of free uranyl. More details on this specific mechanism of uranium sorption and eventual implications in environmental conditions are discussed in the last section (4.2).

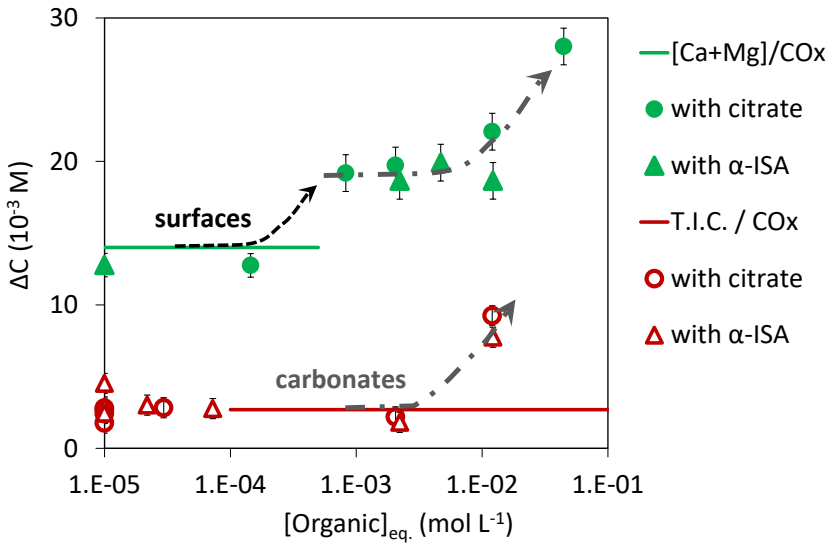

Fig. 5. Disturbance of carbonates chemistry in aqueous solution.
Solid lines: theoretical values in COx clay rock (pH ~ 7.2) in absence of organic compounds.
Signs: Experimental data measured on COx clay rock in presence of citrate and α-ISA.

4. Discussion

4.1. Analogy between Eu(III) and trivalent actinides (Am/Cm/Pu).

Given the similar hydrolysis and complexation constants for Eu(III) and Am(III) in solution (Hummel et al., 2005), similar sorption data are expected: R_d(Am(III)/COx) ~ R_d(Eu(III)/COx) ~ 3.10^4 to 2.10^5 L kg^{-1}. However, surface complexation constants for Am(III) and Eu(III) with the 2SPNE SC/CE model differ depending on the reference, especially for the formation of Clay_sOCm/Am/Eu^{2+} surface species. Bradbury et al. (2005) reported equal log K values (3.1) for Eu(III) and Cm(III), in agreement with further work on Am(III) (Bradbury and Baeyens, 2009a). By using this parameters set and Eu(III) as analogue of Pu(III), sorption and redox speciation of Pu(III/IV) at illite surface could be predicted accurately (Banik et al., 2016; Marsac et al., 2017), which further highlights the reliability of this parameters set. However, Bradbury and Baeyens (2009a, 2011) reported another value of 1.9 for Eu(III), strongly differing from Am/Cm(III) value (Table 2). This second parameters set could not reproduce our sorption data on COx clay rock, even with a high estimate of illite content in COx sample, i.e. over 50%. The parameter set proposed by Bradbury et al. (2005) was therefore taken into account in the present work.

The Figure 6 shows the comparison between experimental Eu(III) adsorption data and predictive modelling on Am(III), i.e. using Am(III) sorption and speciation constants in the model. The agreement between data also validates the analogy between both elements. The value of the plateau illustrates the similar surface complexation constants for Am(III) and Eu(III). The values of concentrations edges in presence of organic compounds also indicate similar complexation constants in solution for Am(III) and Eu(III). The corresponding analogies and values selected in *ThermoChimie* TDB are listed in Table 3.

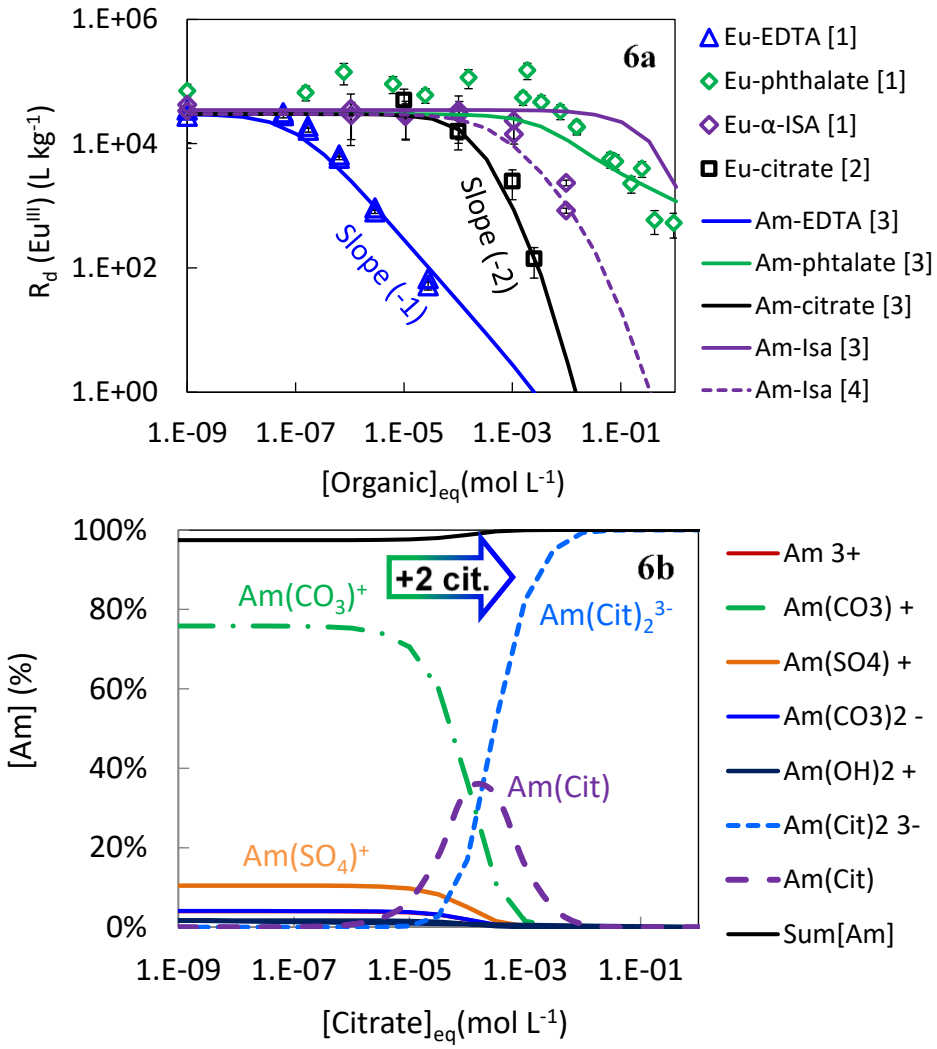

Fig. 6. (6a) Experimental Eu(III) sorption data (signs) compared to predictive model on Am(III) (solid lines). (6b) Speciation of americium in COx pore water as a function of citrate concentration. [1] This study [2] Schott et al., (2012) on Opalinus clay
[3] Predictive model using Am(III) sorption data and *ThermoChimie* TDB.
[4] Model with Am-ISA complexation constant adjusted by analogy with Eu-ISA (this work).

A value of $\log_{10}\beta°(Am(EDTA)^-)$ = 19.67 and values of $\log_{10}\beta°_1(Am(Citrate))$ = 8.55 and $\log_{10}\beta°_2(Am(Citrate))$ = 13.9 are selected in TDB based on data from (Hummel et al., 2005). All these values predict accurately the concentration edges observed for europium. This agreement strengthen other values for Eu(III) selected by analogy with Am(III). The $Am(o\text{-phthalate})^+$ complex reported in *ThermoChimie* TDB is already based on an analogy with Cm(III) (Panak et al., 1995). This corresponds to a complexation constant $\log_{10}\beta°_1(Cm/Am(o\text{-phthalate})^+)$ = 4.93 close to $\log_{10}\beta°_1(Eu(o\text{-phthalate})^+)$ = 4.96. No complexation data for $Am(o\text{-phthalate})_2^-$ is reported in *ThermoChimie* TDB and no Am(III) diphthalate complex is expected in operational disposal conditions, as shown for Eu(III). Finally, Am-ISA complex was only reported at high pH (Tits et al., 2005). Given the analogy between sorption data of both elements, we suggest a similar complexation for Am(III) with a value $\log_{10}\beta°(Am(HISA)^-) \sim \log_{10}\beta°(Eu(HISA)^-) \sim -16.3 \pm 0.3$ (Table 3). The systems with Cm(III)/Pu(III) are outside the scope of the present article, but similar methodology may be applied, given the analogies on aqueous complexation constants.

4.2. Effect of media and U(VI) sorption mechanism

In order to assess the disturbance by organic compounds in other environmental media, complementary experiments were performed on the decarbonated material. A disturbance of uranium sorption in calcite free systems is expected within organic plumes through two antagonistic effects: on one hand the "decomplexation" of U(VI)/Ca/CO_3^{2-} complexes due to free calcium depletion, and on the other hand, the formation of U(VI)-Organic complexes. Analogue effects are evidenced using molecular modelling approaches on cementitious materials by Androniuk and Kalinichev (2020), with gluconate forming stable complexes with Ca^{2+}, thus promoting the substitution of Ca^{2+} by Ca-uranyl complexes. Figure 7a shows the disturbance of [T.I.C.] and pH in presence of highly complexing compound, i.e. citrate.

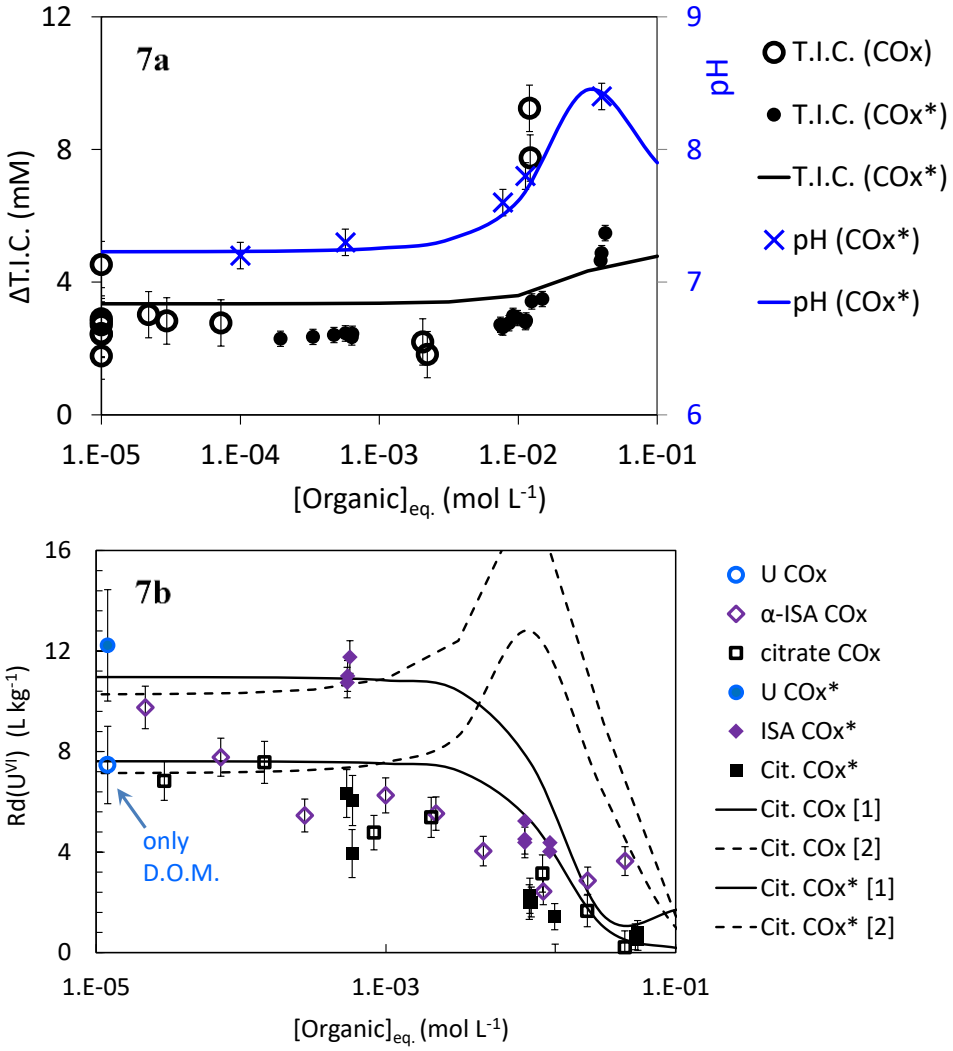

Fig. 7. Comparison of U(VI) sorption data between COx and decarbonated COx samples (noted COx*). (7a) Experimental data and predictive model of COx / Citrate system chemistry. (7b) U(VI) raw sorption data (noted only D.O.M.) and with addition of α-ISA or citrate. Solid lines ([1]): model with the parameter $\log_{10}K_1°(Clay\_sOUO_2(CO_3)^-)$ adjusted.
Dashed lines ([2]): model with the parameter $\log_{10}K_2°(Clay\_sOUO_2(CO_3)_2^{3-})$ adjusted.

A disturbance of speciation is observed above [citrate] > 10^{-2} M. The experimental data is in agreement with a model including equilibrium with low amounts of calcite (< 0.5%). This result shows

that the "decarbonated" samples may be still reactive to organic plume, even with low content of carbonates remaining after strong acid treatment, i.e. less than 0.3% remaining out of 30% initially. Figure 7b shows the corresponding sorption data in presence of citrate and α-ISA. An increase of R_d(U(VI)/COx) is observed, from 7.5 ± 1.6 L kg^{-1} for COx, up to 12.2 ± 0.6 L kg^{-1} for the decarbonated sample. This increase is in agreement with a mass loss of sample, after removal of 30-35% of carbonates. In absence of organic compounds, the ternary complexes U(VI)/Ca/CO_3 are predominant, inducing low R_d values. When increasing [Organic], free Ca^{2+} is depleted leading to the decomplexation of U(VI)/Ca/CO_3 complexes (Fig. 4b). However, this decomplexation does not necessarily increase the sorption of uranium in natural media with low carbonate content, as expected in totally carbonate free systems.

Experimental data on decarbonated samples displays an interesting feature, regarding of the shape of sorption isotherm. As previously discussed, some controversies subsist regarding the microscopic mechanism of uranium sorption in presence of carbonates (Tournassat et al., 2017). Sorption of monocarbonato or dicarbonato uranyl complex are hypotheses, eventually considered (Maia, 2018; Marques Fernandes et al. 2012), or not (Marques Fernandes et al., 2015; Tournassat, 2017), on clay-rich media. The impact of these hypotheses on modelling is illustrated in Fig. 7b. Interestingly, the shape of sorption isotherm strongly depends on the mechanism of the sorption process. By considering monocarbonato-uranyl surface complex (Fig. 7b, solid lines), a constant decrease of R_d(U(VI)/COx) is expected while increasing citrate concentration. By considering dicarbonato-uranyl surface complex, an increase of R_d(U(VI)/COx) value is expected in a narrow range of citrate concentration around 10^{-2} M, before the decrease of sorption (Fig. 7b, dashed lines). The experimental data seems in better agreement with the first hypothesis, regardless of the material used (raw or decarbonated sample), or the organic compound (citrate of α-ISA). Still, such assumption should be taken cautiously and complementary investigations (TRLS, FTIR, or XAS spectroscopies) are mandatory in order to strengthen mechanistic modelling.

5. Conclusion

In this work, the retention of Eu(III), Th(IV), U(VI), was quantified and modelled in presence of small organic acids. Adsorption isotherms of RNs were acquired on Callovo-Oxfordian clay rock as a function of concentration of various carboxylic acids. A simplified surface complexation model, taking into account strong sorption sites for illite, describes accurately the sorption on such natural media. The organic concentration edges, above which the complexation by organic compounds becomes predominant are quantified. This allows the assessment of the sorption model and of the thermodynamic database developed by the consortium Andra-RWM-Ondraf: ThermoChimie (V10a). A wide range of concentrations of organic compounds was studied in this work, above operational conditions of radioactive waste disposal context. These data are then useful for better understanding of RN migration in sedimentary rocks.

Various organic concentration edges were quantified for Eu(III) and Th(IV), from 10^{-7} up to 1 M, above which the complexation of RNs by organic acids leads to a decrease of sorption. These concentration edges depend on the nature of the organic compound and its selectivity towards the RNs in the environmental conditions. Predictive modelling agrees with experimental data and confirms the robustness of the surface complexation model to account for surface speciation, and of the thermodynamic database to account for speciation in solution. Some thermodynamic data on organic systems from *ThermoChimie* TDB were reviewed. The evaluation of complexation constant $\log_{10}\beta°(Eu(OH)_{3-x}(H_{4-x}(\alpha\text{-ISA}))^{-})$ = -16.3 ± 0.3, possibly indicates a new mechanism at neutral pH, deserving further spectroscopic investigation. The retention of Th(IV) in presence of citrate also

indicates an additional mechanism, possibly with a sorption of $Th(Cit)^{+}$, and deserves further investigation as well. As for other RNs, a decrease of U(VI) retention on clay rock is observed in presence of organic compounds. Yet, the underlying mechanism strongly differs from that for Eu(III) and Th(IV). The inorganic ions released along with the organic plume, Ca^{2+}, Mg^{2+}, CO_3^{2-}, are complexing species of U(VI), thus decreasing its sorption. Hence, this disturbance by organic compounds is less sensitive to the nature of the organic compounds, as the chemical equilibrium is mostly displaced when the concentration of carboxylate functions exceeds the available stock of divalent cations and affects the solubility of carbonate minerals.

These results have implications on the models describing RNs migration in the environment, and more generally in presence of organic plumes. In specific cases of RNs complexation with calcium, such as for uranium, the nature of the organic compounds may be less important than the buffering effects of dissolved cations and clay surfaces. It is interesting to note that a media buffered at neutral pH in contact with an organic plume at similar pH, may still endure pH drift due to the release of anionic bases (carbonates, phosphates, etc.), even in presence of low amounts of carbonate minerals, i.e. below 1%. As a corollary, the accessibility to carbonate minerals may be more important than its content, regarding specific effect during near-field disturbances. Still, the ratio between the mass of rock and the volume of organic leachate, remains a key factor in order to assess the disturbances in environmental media.

Acknowledgments

This work was financed by the Atomic Energy and Alternative Energies Commission (CEA, Université Paris-Saclay), and by the French national radioactive waste management agency (Andra). Discussion with J.-C. Robinet (Andra) during proposal and interpretation of experiments greatly improved this work. We thank M. Descostes, J. Poonoosamy, I. Pointeau and J. Klein, for early experiments on europium. The help of Serge Lefèvre for ICP-MS measurements and of Nathalie Coreau for ionic chromatography was greatly appreciated. The meticulous read-through and constructive comments of two anonymous reviewers were greatly appreciated. In memory of Eric Giffaut (Andra).

References

Altmann, S., Tournassat, C., Goutelard, F., Parneix, J.-C., Gimmi, T., Maes, N., 2012. Diffusion-driven transport in clayrock formations. Applied Geochem. 27, 436–478.

Andra, Dossier 2005 Argile, Synthesis. Evaluation of the Feasibility of a Geological Repository in an Argillaceous Formation. Meuse/Haute-Marne site; Andra Report series 266.

Androniuk, I., Kalinichev, A.G., 2020. Molecular dynamics simulation of the interaction of uranium VI. with the C–S–H phase of cement in the presence of gluconate. Applied Geochem. 113, 104496.

Bagnoud, A., de Bruijn, I., Andersson, A.F., Diomidis, N., Leupin, O.X., Schwyn, B., Bernier-Latmani R., 2016. Aminimalistic microbial food web in an excavated deep subsurface clay rock. FEMS Microbiology Ecology, 92, fiv138.

Banik, N.L., Marsac, R., Lützenkirchen, J., Diascorn, A., Bender, K., Marquardt, C.M., Geckeis, H., 2016. Sorption and Redox Speciation of Plutonium at the Illite Surface. Environ. Sci. Technol. 50, 2092–2098.

Bauer, A., Rabung, T., Claret, F., Schafer, T., Buckau, G., Fanghnel, T., 2005. Influence of temperature on sorption of europium onto smectite: The role of organic contaminants. Applied Clay Science 30, 1–10.

Bernhard, G., Geipel, G., Reich, T., Brendler, V., Amayri, S., and Nitsche, H., 2001. Uranyl(VI) Carbonate Complex Formation: Validation of the Ca2UO2CO3.3aq. Species. Radiochimica Acta, 89, 511–518.

Besançon, C., Chautard, C., Beaucaire, C., Savoye, S., Sardini, P., Gérard, M., Descostes, M. 2020. The Role of Barite in the Post-Mining Stabilization of Radium-226: A Modeling Contribution for Sequential Extractions. Minerals 10, 497.

Bradbury, M.H., Baeyens, B., 1997. A mechanistic description of Ni and Zn sorption on Na-montmorillonite Part II: modelling. J. Contam. Hydrol. 27, 223–248.

Bradbury, M.H., Baeyens, B., 2002. Sorption of Eu on Na- and Ca-montmorillonites: experimental investigations and modelling with cation exchange and surface. Geochim. Cosmochim. Acta 66, 13, 2325–2334.

Bradbury, M.H., Baeyens, B., Geckeis, H., Rabung, T., 2005a. Sorption of Eu(III)/Cm(III) on Ca-montmorillonite and Na-illite. Part 2: surface complexation modelling. Geochimica et Cosmochimica Acta 69, 5403–5412.
Bradbury, M.H., Baeyens, B., 2005b. Modelling the sorption of Mn(II), Co(II), Ni(II), Zn(II), Cd(II), Eu(III), Am(III), Sn(IV), Th(IV), Np(V) and U(VI) on montmorillonite: linear free energy relationships and estimates of surface binding constants for some selected heavy metals and actinides. Geochim. Cosmochim. Acta 69, 875–892.
Bradbury, M.H., Baeyens, B., 2005c. Investigations on Na-illite: Acid-Base Behaviour and the Sorption of Strontium, Nickel, Europium and Uranyl. Technical Report NTB 05–02, ISSN 1019-0643, Nagra, Wettingen.
Bradbury, M.H., Baeyens, B., 2009a. Sorption modelling on illite. Part I: titration measurements and sorption of Ni(II), Co(II), Eu(III), and Sn(IV). Geochim. Cosmochim. Acta 73, 990–1003.
Bradbury, M.H., Baeyens, B., 2009b. Sorption modelling on illite. Part II: actinide sorption and linear free energy relationships. Geochim. Cosmochim. Acta 73, 1004–1013.
Charlet, L., Alt-Epping, P., Wersin, P., Gilbert, B., 2017. Diffusive transport and reaction in clay rocks: A storage nuclear waste, CO2, H2., energy shale gas. and water quality issue. Advances Water Ress. 106, 39-59.
Chautard, C., Beaucaire, C., Gérard, M., Roy, R., Savoye, S., Descostes, M., 2020. Geochemical characterization of uranium mill tailings Bois Noirs Limouzat, France. highlighting the U and 226Ra retention. J. Envir. Radioact. 218, 106251.
Chen, Z., Montavon, G., Ribet, S., Guo, Z., Robinet, J.C., David, K., Tournassat, C., Grambow, B., Landesman, C., 2014. Key factors to understand in-situ behavior of Cs in Callovo–Oxfordian clay-rock (France). Chem. Geol. 387, 47–58.
Choppin, G.R., Erten, H. N., Xia, Y.-X., 1996. Variation of stability constants of thorium citrate complexes with ionic strength. Radiochim. Acta 74, 123–127.
Colàs, E., Grivé, M., Rojo, Isabel, Duro, L., 2013. The Effect of Gluconate and EDTA on Thorium Solubility Under Simulated Cement Porewater Conditions. J. Solution Chem. 42, 1680–1690.
Dagnelie, R.V.H., Descostes, M., Pointeau, I., Klein, J., Grenut, B., Radwan, J., Lebeau, D., Georgin, D., Giffaut, E., 2014. Sorption and diffusion of organic acids through clayrock: comparison with inorganic anions. J. Hydrol. 511, 619–627.
Dagnelie, R.V.H., Arnoux, P., Radwan, J., Lebeau, D., Nerfie, P., Beaucaire, C., 2015. Perturbation induced by EDTA on HDO, Br- and Eu(III) diffusion in a large-scale clay rock sample. Appl. Clay Sci. 105–106, 142–149.
Dagnelie, R.V.H., Arnoux, P., Enaux, J., Radwan, J., Nerfie, P., Page, J., Coelho, D., Robinet, J.-C., 2017. Perturbation induced by a nitrate plume on diffusion of solutes in a large-scale clay rock sample. Appl. Clay Sci. 141, 219–226.
Dagnelie, R.V.H., Rasamimanana, S., Blin, V., Radwan, J., Thory, E., Robinet, J.-C., Lefèvre, G., 2018. Diffusion of Organic Anions in Clay-Rich Media: Retardation and Effect of Anion Exclusion. Chemosphere 213, 472–480.
Descostes, M., Blin, V., Bazer-Bachi, F., Meier, P., Grenut, B., Radwan, J., Schlegel, M.L., Buschaert, S., Coelho, D., Tevissen, E., 2008. Diffusion of anionic species in Callovo-Oxfordian argillites and oxfordian limestones Meuse/Haute-Marne, France. Appl. Geochem. 23, 655–677.
Descostes, M., Pointeau, I., Radwan, J., Poonoosamy, J., Lacour, J.-L., Menut, D., Vercouter, T., Dagnelie, R.V.H., 2017. Adsorption and retarded diffusion of Eu(III)-EDTA- through hard clay rock. J. Hydrol. 544,125–132.
Dong, W.M., Brooks, S.C., 2006. Determination of the Formation Constants of Ternary Complexes of Uranyl and Carbonate with Alkaline Earth Metals Mg2+, Ca2+, Sr2+, and Ba2+. Using Anion Exchange Method. Environ. Sci. Technol. 40, 4689–4695.
Dublet, G., Lezama Pacheco, J., Bargar, J.R., Fendorf, S., Kumar, N., Lowry, G.V., Brown, G.E., 2017. Partitioning of uranyl between ferrihydrite and humic substances at acidic and circum-neutral pH. Geochim. Cosmochim. Acta 215, 122–140.
Dudás, C., Kutus, B., Böszörményi, É., Peintler, G., Kele, Z., Pálinkó, I., Sipos, P., 2017. Comparison of the Ca2+ complexing properties of isosaccharinate and gluconate – is gluconate a reliable structural and functional model of isosaccharinate? Dalton Trans. 46, 13888–13896.
Felmy, A.R., Cho, H., Dixon, D.A., Xia, Y., Hess, N.J. and Wang, Z., 2006. The aqueous complexation of thorium with citrate under neutral to basic conditions. Radiochim. Acta 94, 4, 205–212.
Gao, Y., Shao, Z., and Xiao, Z., 2015. UVI. Sorption on Illite: Effect of pH, Ionic Strength, Humic Acid and Temperature. J. Radioanal. Nuclear Chem. 303, 1, 867-876.
Gaucher, E., Robelin, C., Matray, J., Negrel, G., Gros, Y., Heitz, J., Vinsot, A., Rebours, H., Cassagnabère, A., Bouchet, A., 2004. ANDRA underground research laboratory: interpretation of the mineralogical and geochemical data acquired in the Callovo-Oxfordian formation by investigative drilling. Phys. Chem. Earth 29, 55–77.
Geoffroy, C., Foissy, A., Persello, J., Cabane, B., 1999. Surface Complexation of Calcite by Carboxylates in Water, J. Coll. Interf. Sci. 211, 45–53.
Giffaut, E., Grivé, M., Blanc, P., Vieillard, P., Colàs, E., Gailhanou, H., Gaboreau, S., Marty, N., Madé, B. and Duro, L., 2014. Andra thermodynamic database for performance assessment: ThermoChimie. Applied Geochem. 49, 225–236.

Glaus, M.A., van Loon; L.R., Achatz, S.Codura, A., Fischer, K., 1999. Degradation of cellulosic materials under the alkaline conditions of a cementitious repository for low and intermediate level radioactive waste: Part I: Identification of degradation products. Analytica Chimica Acta 398, 111–122.
Glaus, M.A., Baeyens, B., Lauber, M., Rabung, T. and Van Loon, L.R., 2005. Influence of water-extractable organic matter from Opalinus Clay on the sorption and speciation of Ni(II), Eu(III) and Th(IV). Applied Geochem. 20, 443–451.
Grasset, L., Brevet, J., Schäfer, T., Claret, F., Gaucher, E.C., Albrecht, A., Amblès, A., 2010. Sequential extraction and spectroscopic characterisation of organic matter from the Callovo-Oxfordian formation. Organic Geochem. 41, 221–233.
Grenthe, I., Gaona, X., Plyasunov, A.V., Rao, L., Runde, W.H., Grambow, B., Konings, R.J.M., Smith, A.L., Moore, E.M., 2020. Vol. 14. Second update on the chemical thermodynamics of Uranium, Neptunium, Plutonium, Americium and Technetium, OECD Nuclear Energy Agency Data Bank, Eds., OECD Publications, Paris, France, (2020).
Hongxia, Z., Xiaoyun, W., Honghong, L., Tianshe, T., Wangsuo, W., 2016. Adsorption behavior of Th(IV) onto illite: Effect of contact time, pH value, ionic strength, humic acid and temperature. Applied Clay Sci. 127–128, 35–43.
Huclier-Markai, S., Landesman, C., Rogniaux, H., Monteau, F., Vinsot, A., Grambow, B., 2010. Non-disturbing characterization of natural organic matter NOM. contained in clay rock pore water by mass spectrometry using electrospray and atmospheric pressure chemical ionization modes. Rapid Commun. Mass Spectrom. 24, 191–202.
Hummel, W., Anderegg, G., Rao, L., Puigdomènech, I., Tochiyam, O., 2005. Chemical Thermodynamics. Vol. 9. Chemical Thermodynamics of Compounds and Complexes of U, Np, Pu, Am, Tc, Se, Ni and Zr with Selected Organic Ligands OECD Nuclear Energy Agency, ed. Elsevier.
Jo, Y., Lee, J.Y., Yun, J.I., 2018. Adsorption of uranyl tricarbonate and calcium uranyl carbonate onto γ-alumina. Applied Geochem. 94, 28–34.
Joseph, C., Schmeide, K., Sachs, S., Brendler, V., Geipel, G., Bernhard, G., 2011. Sorption of uranium(VI) onto Opalinus Clay in the absence and presence of humic acid in Opalinus Clay pore water. Chem. Geol. 284, 240–250.
Joseph, C., Stockmann, M., Schmeide, K., Sachs, S., Brendler, V., Bernhard, G., 2013. Sorption of UVI. onto Opalinus Clay: Effects of pH and humic acid. Applied Geochem. 36, 104–117.
Kalmykov, S .N, Choppin, R. 2009. Mixed Ca2+/UO22+/CO32- complex formation at different ionic strengths. Radiochimica Acta 88, 603-606.
Kautenburger, R., Brix, K., Hein, C., 2019. Insights into the retention behaviour of europium(III) and uranium(VI) onto Opalinus Clay influenced by pore water composition, temperature, pH and organic compounds. Applied Geochem. 109, 104404.
Lerouge, C., Grangeon, S., Gaucher, E.C., Tournassat, C., Agrinier, P., Guerrot, C., Widory, D., Fléhoc, C., Wille, G., Ramboz, C., 2011. Mineralogical and isotopic record of biotic and abiotic diagenesis of the Callovian–Oxfordian clayey formation of Bure France. Geochim. Cosmochim. Acta 75, 2633–2663.
Ma, B., Charlet, L., Fernandez-Martinez, A., Kang, M., Madé, B., 2019. A review of the retention mechanisms of redox-sensitive radionuclides in multi-barrier systems. Applied Geochem. 100, 414-431.
Maia, F., 2018. Impact de l'élévation de la température jusqu'à 80°C sur le comportement des radionucléides dans le Callovo-Oxfordien : application à l'uranium. PhD Thesis, 2018IMTA0078. Université IMT Atlantique.
Marques Fernandes, M., Baeyens, B., Dähn, R., Scheinost, A.C. and Bradbury, M.H., 2012. U(VI) sorption on montmorillonite in the absence and presence of carbonate: a macroscopic and microscopic study. Geochim. Cosmochim. Acta 93, 262–277.
Marques Fernandes, M., Vér, N., Baeyens, B., 2015. Predicting the uptake of Cs, Co, Ni, Eu, Th and U on argillaceous rocks using sorption models for illite. Applied Geochem. 59, 189–199.
Marsac, R., Banik, N.L., Lützenkirchen, J., Diascorn, A., Bender, K., Marquardt, C.M., Geckeis, H., 2017. Sorption and redox speciation of plutonium at the illite surface under highly saline conditions. J. Coll. Interf. Sci. 485, 59–64.
Martin, L.A., Wissocq, A., Benedetti, M.F., Latrille, C., 2018. Thallium Tl. sorption onto illite and smectite: Implications for Tl mobility in the environment. Geochim. Cosmochim. Acta 230, 1–16.
McCarthy, J.F., Sanford, W.E., Stafford, P.L., 1998. Lanthanide field tracers demonstrate enhanced transport of transuranic radionuclides by natural organic matter. Environ. Sci. Technol. 32, 3901–3906.
Melkior, T., Yahiaoui, S., Thoby, D., Motellier, S., Barthes, V., 2007. Diffusion coefficients of alkaline cations in Bure mudrock. Phys. Chem. Earth 32, 453–462.
Motellier, S., Ly, J., Gorgeon, L., Charles, Y., Hainos, D., Meier, P., Page, J., 2003. Modelling of the ion-exchange properties and indirect determination of the interstitial water composition of an argillaceous rock. Application to the Callovo-Oxfordian low-water-content formation. Appl. Geochem. 18, 1517–1530.
Pabalan, R.T., Turner, D.R., 1996. Uranium(6+) Sorption on Montmorillonite: Experimental and Surface Complexation Modeling Study. Aquatic Geochem. 2, 203–226.

Parkhurst, D., Appelo, C. 2013. Description of input and examples for PHREEQC version 3. A Computer Program for Speciation, Batch-reaction, One-Dimensional Transport, and Inverse Geochemical Calculations, U.S. Geological Survey Techniques and Methods 6, A43.
Panak, P., Klenze, R., Kim, J., 1995. A study of intramolecular energy transfer in Cm(III) complexes with aromatic ligands by time-resolved laser fluorescence spectroscopy. J. Alloys and Compounds 225, 261–266.
Pellenard, P., Deconinck, J.-F., 2006. Mineralogical variability of Callovo-Oxfordian clays from the Paris Basin and the Subalpine Basin. C.R. Geoscience 338, 854-866.
Peynet, V. 2003. Rétention d'actinides et de produits de fission par des phases polyminérales. PhD Thesis, Paris VI University.
Rand, M., Fuger, J., Grenthe, I., Neck, V., Rai, D., 2009. Chemical thermodynamics of thorium. OECD Nuclear Energy Agency Data Bank, 11, Eds., OECD Publications, Paris, France.
Rai, D., Yui, M., Moore, D.A., Rao, L., 2009. Thermodynamic model for ThO2am. solubility in isosaccharinate solutions. J. Solution Chem. 38, 1573–1587.
Rasamimanana, S., Lefèvre, G., Dagnelie, R., 2017. Adsorption of polar organic molecules on sediments : case-study on Callovian-Oxfordian claystone. Chemosphere 181, 296–303.
Read, D., Ross, D. and Sims, R.J., 1998. The migration of uranium through Clashach Sandstone: the role of low molecular weight organics in enhancing radionuclide transport. J. Contam. Hydrol. 35, 235–248.
Reinoso-Maset, E., Ly, J., 2014. Study of major ions sorption equilibria to characterize the ion exchange properties of kaolinite. J. Chem. Eng. Data 59, 4000–4009.
Reinoso-Maset, E., Ly, J., 2016. Study of uranium(VI) and radium(II) sorption at trace level on kaolinite using a multisite ion exchange model. J. Envir. Radioact. 157, 136–148.
Rout, S.P., Charles, C.J., Garratt, E.J., Laws, A.P., Gunn, J., Humphreys, P.N., 2015. Evidence of the Generation of Isosaccharinic Acids and Their Subsequent Degradation by Local Microbial Consortia within Hyper-Alkaline Contaminated Soils, with Relevance to Intermediate Level Radioactive Waste Disposal. Plos One 10, 3, e0119164.
Schott, J., Acker, M., Barkleit, A., Brendler, V., Taut, S., Bernhard, G., 2012. The influence of temperature and small organic ligands on the sorption of Eu(III) on Opalinus Clay. Radiochim Acta 100, 315–324.
Semenkova, A.S., Evsiunina, M.V., Verma, P.K., Mohapatra, P.K., Petrova, V.G., Seregina, I.F., Bolshova, M.A., Krupskaya, V.V., Romanchuka, A.Y., Kalmykova, S.N., 2018. Cs+ sorption onto Kutch clays: Influence of competing ions. Applied Clay Sci. 166, 88–93.
Shang, C., Reiller, P.E., 2020. Determination of formation constants and specific ion interaction coefficients for CanUO2CO3.34−2n.− complexes in NaCl solution by time-resolved laser-induced luminescence spectroscopy. Dalton Trans 2, 49, 466–481.
Shaw, Paul B., 2013. Studies of the Alkaline Degradation of Cellulose and the Isolation of Isosaccharinic Acids. Doctoral thesis, University of Huddersfield.
Tasi, A., Gaona, X., Fellhauer, D., Böttle, M, Rothe, J., Dardenne, K., Polly, R., Grivé, M., Colàs, E., Bruno, J., Källström, K., Altmaier, M., Geckeis, H., 2018. Applied Geochem. 98, 247–264.
Tertre, E., Beaucaire, C., Coreau, N., Juery, A., 2009. Modelling Zn(II) sorption onto clayey sediments using a multi-site ion-exchange model. Applied Geochem. 24, 1852-1861.
Tits, J., Wieland, E., Bradbury, M.H., Eckert, P., Schaible, A., 2002. The Uptake of Eu(III) and Th(IV) by Calcite Under High pH Cement Pore Water Conditions. PSI Report 02-03, Paul Scherrer Institut, Villigen, Switzerland and Nagra, Technical Report NTB 02-08, Nagra, Wettingen, Switzerland.
Tits, J., Wieland, E., Bradbury, M.H. 2005. The effect of isosaccharinic acid and gluconic acid on the retention of Eu(III), Am(III) and Th(IV) by calcite. Applied Geochem. 20, 2082–2096.
Tournassat, C., Grangeon, S., Leroy, S., Giffaut, E., 2013. Modelling specific pH dependent sorption of divalent metals on montmorillonite surfaces. A review of pitfalls, recent achievements and current challenges. Am. J. Sci. 313, 395-451.
Tournassat, C., Tinnacher, R.M., Grangeon, S., Davis, J.A., 2017. Modelling uranium(VI) adsorption onto montmorillonite under varying carbonate concentrations: A surface complexation model accounting for the spillover effect on surface potential. Geochim. Cosmochim. Acta 220, 291–308.
Troyer, L.D., Maillot, F., Wang, Z., Wang, Z., Mehta , V.S., Giammar, D.E., Catalano, J.G., 2016. Effect of phosphate on U(VI) sorption to montmorillonite: Ternary complexation and
precipitation barriers. Geochim. Cosmochim. Acta 175, 86–99.
Van Loon, L.R., Glaus, M.A., 1998. Experimental and Theoretical Studies on Alkaline Degradation of Cellulose and its Impact on the Sorption of Radionuclides. PSI Report 98-07,
Paul Scherrer Institut, Villigen, Switzerland and Nagra Technical Report NTB 97-04, Nagra, Wettingen, Switzerland.
Van Loon, Glaus, M.A., Laube, A., Stallone, S., 1999. Degradation of cellulosic materials under the alkaline conditions of a cementitious repository for low and intermediate level radioactive waste: Part III: Effect of Degradation Products on the Sorption of Radionuclides on Feldspar. Radiochim. Acta 86, 183–189.

Vercammen, K., Glaus, M.A., Van Loon, L.R., 2001. Complexation of Th(IV) and Eu(III) by α-isosaccharinic acid under alkaline conditions. Radiochim. Acta 89, 393-401.
Verma, P.K., Semenkova, A.S., Krupskaya, V.V., Zakusin, S.V., Mohapatra, P.K., Romanchuk, A.Y., Kalmykov, S.N., 2019. Eu(III) sorption onto various montmorillonites: Experiments and modelling. Applied Clay Sci. 175, 22–29.
Vu-Do, L., 2011. Influence of Natural Mobile Organic Matter on Europium Retention on Bure Clay Rock. Ph.D. Thesis. Université d'Orsay Paris-XI, France.
Whistler, R. L., BeMiller, J. N., 1963. α-D-Isossacharino-1,4-Lactone. In Methods in Carbohydrate Chemistry, Vol. 2 Reactions of Carbohydrates; Wolfrom, M. L., BeMiller, J. N., Eds.; Academic Press: New York, 477–479.
Wissocq, A., Beaucaire, C., Latrille, C., 2018. Application of the multi-site ion exchanger model to the sorption of Sr and Cs on natural clayey sandstone. Applied Geochem. 93, 167–177.

APPENDIX: Supplementary material for

Effect of organic compounds on the retention of radionuclides in clay rocks: Mechanisms and specificities between Eu(III), Th(IV), and U(VI).

Lizaveta Fralova[(a)], Grégory Lefèvre[(b)], Benoît Madé[(c)], Rémi Marsac[(d)], Emilie Thory[(a)], Romain V.H. Dagnelie[(a)]

[a] Université Paris-Saclay, CEA, Service d'Etude du Comportement des Radionucléides, 91191, Gif-sur-Yvette, France

[b] PSL Research University, Chimie ParisTech-CNRS, Institut de Recherche de Chimie Paris, 11 rue Pierre et Marie Curie, F-75005 Paris, France

[c] Andra, R&D Division, parc de la Croix Blanche, 92298, Châtenay-Malabry, France

[d] Univ. Rennes, CNRS, Géosciences Rennes - UMR 6118, F-35000 Rennes, France

Table S1. Properties of retention experiments in this study. Ref. 1 : The order of adding follows: clay sample / pore water / organic solution / RN. Ref. 2: Half of pore water ($V_0/2$) was added to the clay for equilibration during a week, before previous protocol (Ref. 1). **ISA mixed with other compounds, similar concentrations for α-ISA, acetate, o-phthalate, glutarate and 10^{-5} mol L^{-1} of oxalate. *ISA: mixture of α-, β-ISA (purified salt) and mixture of α- β- and x-ISA isomers (raw lixiviate) from cellulose degradation in $Ca(OH)_2$ (Shaw, 2013).

RN	Organic	Experiment (n°)	COx (sample)	$[RN]_0$ (mol/L)	V (mL)	m (g)	V/m (L/kg)	A_0 (kBq)	Tads. (days)	Adding Order	Comments
Eu	EDTA	E1-12	EST207 16517 (-502 m)	(2±1)E-8	9	0.1	90	5	1	Ref. 1	From Descostes et al., 2017
	α-ISA	I1-12			9	0.1	90	5	1	Ref. 1	
	o-phthalate	P1-P10		(1.7±0.1)E-8	20	0.25	80	8	1	Ref. 1	$[phthal.]_0$ < 1.5 E-2 mol L^{-1}
	o-phthalate	P12-P21		(1.2±0.1)E-8	40	0.1	400	5	1	Ref. 1	$[phthal.]_0$ = 1E-3 - 0.3 mol L^{-1}
	oxalate	O1-O10		(1.7±0.1)E-8	20	0.25	80	8	1	Ref. 1	
	acetate	A1-A10		(1.7±0.1)E-8	20	0.25	80	8	1	Ref. 1	
	EDTA	JP1-JP10		(0.8±0.1)E-8	40	0.15	267	6	1	Ref. 1	
	α-ISA**	U_S1-S4	EST45988 (-489 m)	(0.8 to 10)E-8	37	0.1	370	5	7	Ref. 1	ISA with other compounds**
Th	citrate	Cit1-15	EST51764 (-477 m)	(4.3±0.1)E-6	2	0.1	20	^{nat}Th	1	Ref. 2	
	α-ISA	ISA1-15		(4.3±0.1)E-6	2	0.1	20		1	Ref. 2	
	o-phthalate	P1-P15		(4.3±0.1)E-6	2	0.1	20			Ref. 2	
	α-ISA**	Th_S1-S4	EST45988	(2 to 3) E-8	35	0.014	2500		7	Ref. 1	ISA with other compounds**
U	citrate	U1_1-15	EST51775 (-471 m)	(4.8±0.2)E-7	2	0.2	10	^{nat}U	1	Ref. 2	
	α-ISA	U1_16-30		(4.8±0.2)E-7	2	0.2	10		1	Ref. 2	
	o-phthalate	U2_1-15		(5.3±0.15)E-7	2	0.2	10		1	Ref. 2	
	succinate	U2_16-30		(5.3±0.15)E-7	2	0.2	10		1	Ref. 2	
	o-phthalate*	U1_31-34		(5.3±0.15)E-7	2	0.2	10		1	Ref. 2	
	β,α,x-ISA*	ISA_1-21		(1.5±0.1)E-7	6	0.5	12		1	Ref. 2	mixture of β-, α-, and x-ISA*

Table S2. Composition of synthetic pore water solutions used (unity is 10^{-3} mol L^{-1})

Species	Na^+	K^+	Ca^+	Mg^+	Sr^+	Cl^-	SO_4^{2-}	Alk.	pH
Synthetic water	46.1	1.03	7.36	6.67	0.20	41.0	15.6	3.34	7.15

Pore water preparation:

The preparation of synthetic pore was performed with the following procedure. Salts of high purity (> 99%) were dissolved in 5L of Milli-Q® water to reach the targeted concentrations of major ions (Table S1). The solution was then bubbled a gas mixture (N_2 with 1% of CO_2) during 30 min in order to remove oxygen and equilibrate pH and $CO_{2(d)}$. The solution was then transferred in anoxic glove box ($P(O_2)/P° << 10$ ppm). Some sacrificial crushed clay rock was added to the pore water with a ratio of 50 g L^{-1}. This suspension was stirred at least during 48h for equilibration of traces elements (Fe, Al, SiO_2, D.O.M.). The solution was then filtered two times (cellulose or nylon filters). The first filtration at 2-5 µm allows removal of sacrificial clay. The second filtration below 0.2 µm is mostly used to prevent bacterial activity. Filtrated solution are collected in 1 L pyrex® glass bottles, filled entirely with pore water, and closed for stored in glovebox. A few days before use of a new bottle, the solution is bubbled again during 30 min (N_2 with 1% CO_2). pH is then measured and eventually adjusted to 7.2 ± 0.2 if necessary. Composition of pore water is controlled by ionic chromatography (850 Professional IC Cation and Anions from Metrohm), except for carbonates. Carbonates are measured by total inorganic carbon measurement with a Vario TIC-TC from Elementar®. Alkalinity is quantified by pH acidic dosage with diluted HCl, or UV-Vis dosage by HCOOH in presence of bromophenol blue (BBP). The synthetic pore water is used furtherly to equilibrate clay rock samples and mineral surfaces by multiple mixing / renew steps, following the protocol developed by Descostes et al., 2004.

Table S3. Name and properties of the studied organic acids.

Formula, Molecular Weight (Mw) and Octanol Water distribution coefficient (POW) correspond to the acidic form (HA).

Species are under anionic form in COx porewater (pH ~ 7.2 >> pKa1).

Studied species (carboxylate: A^-)	IUPAC Name (carboxylic acid: HA)	Formula (HA)	M_w (g mol^{-1})	pKa	Charge pH~7.2	Speciation in COx (% of species)
Acetate	Ethanoic acid	$C_2H_4O_2$	60.05	4.76	$Ac.^-$	$Ac.^-$ / 96.9 $CaAc.^+$ / 2.8
ortho-Phthalate	Benzene-1,2-dioic acid	$C_8H_6O_4$	166.14	2.94, 5.43	$Ph.^{2-}$	$Ph.^{2-}$ / 77.7 CaPh. /21.8
Oxalate	Ethanedioic acid	$C_2H_2O_4$	90.03	1.25, 4.14	$Ox.^{2-}$	MgOx. / 55.9 CaOx. / 25.7 $Ox.^{2-}$ / 18.3
α-Isosaccharinate	(2S,4S)-2,4,5-Trihydroxy-2-(hydroxymethyl)pentanoic acid	$C_6H_{12}O_6$	180.16	4.02	H_4ISA^-	$H_4Isa.^-$ / 89.9 $CaH_4Isa.^+$ / 10.0
Citrate	2-Hydroxypropane-1,2,3-tricarboxylic acid	$C_6H_8O_7$	192.12	3.13, 4.76, 6.40	$Cit.^{3-}$	$CaCit.^-$ / 49.9 $MgCit.^-$ / 47.3 $Cit.^{3-}$ / 2.2
EDTA	2,2′,2″,2‴-(Ethane-1,2-diyldinitrilo)tetraacetic acid	$C_{10}H_{16}N_2O_8$	292.24	0, 1.5, 2, 2.7, 6.2, 10.2	$EDTA^{4-}$	$CaEDTA^{2-}$ / 98.5 $MgEDTA^{2-}$ / 1.5
Succinate	Butane-1,4-dioic acid	$C_4H_6O_4$	118.09	4.2, 5.6	$Succin.^{2-}$	$Succ.^{2-}$ / 72.9 $Ca(Succ.)^{2-}$ / 14.5 $Mg(Succ.)^{2-}$ / 11.4

Table S4. Adsorption parameters of organic molecules.

Taken from Rasamimanana et al. 2017

Molecule	Langmuir parameters		
	K	Q	R_d^{MAX}
	(L mol^{-1})	(mol kg^{-1})	(L kg^{-1})
Acetate	Not available		<< 0.2
Adipate	$8.95\ 10^{2}$	$5.5\ 10^{-4}$	0.18 [0.02-0.3]
Benzoate	Not available		0.2 [0.05-0.3]
Glutarate	$1.1\ 10^{1}$	$4.0\ 10^{-2}$	043 [0.1-0.7]
Phthalate	$1.22\ 10^{3}$	$1.23\ 10^{-3}$	1.53 [1.3-1.7]
Succinate	Not available		3.5 [3.1-3.9]
Oxalate	$C_{sat} \sim 10^{-5}$ M << 1/K		8.4 [7.4-9.4]
Gluconate	Not available		8.8 [6.7-10.9]
EDTA	$4.26\ 10^{1}$	$2.95\ 10^{-1}$	12.4 [6-15]
ISA	$3.47\ 10^{3}$	$8.8\ 10^{-3}$	29 [24-34]
Citrate	$1.19\ 10^{4}$	$4.65\ 10^{-3}$	54.7 [42-70]

Surface complexation model and parameters:

In the main manuscript, Table 2 provides properties of solid samples and surface site used in modelling. The content of minerals in samples was converted in a percentage of pure illite fraction. To that aim, the estimation of Q was performed as follows. A proportion of 20 % of pure illite was considered in the solid sample as measured in experimentally (Gaucher et al., 2004; Lerouge et al., 2011; Pellenard and Deconinck, 2014). An additional 21 % of interstratified illite/smectite (I/S) was calculated, based on the experimental cationic exchange capacity: $CEC_{EXP} = 1.6\ 10^{-1}$ mol kg(COx)$^{-1}$ (measured by exchange K^+ / Cs^+) and in agreements with data from samples at similar geological depth (Andra, 2005). Considering, I/S as a 50/50 mixture of pure illite and pure smectite, this leads to a percentage of illite in COx samples: p = 20 + 0.5×21 = 30.5 % = 0.305 kg(illite)/kg(COx). The site density was taken from strong

surface site, reported for Eu(III) retention on illite in (Bradubury et al., 2005): i.e. [≡S_sOH] = 2 10^{-3} mol kg(illite). For example, with V/m = 100 L kg^{-1} used in some of the Eu(III) experiments, this leads to: Q = p×[≡S_sOH] = 6.1 10^{-4} mol kg(COx)$^{-1}$ for Eu(III) sorption. Site concentration was converted per kg of solution for PhreeqC scripts, using V/m ratio from experiments and solution density d ~ 1.01 kg L^{-1}.

Table S5. Data used for complexation between organic molecules and radionuclides. Complexation constants, $log_{10}K°$ (25°C, I.S. = 0). Values in italic reprocessed at I.S. = 0 using Davies equation. TDB : "ThermoChimie" Database V10a (https://www.thermochimie-tdb.com/). *Value not recommended. ISA: α-isosaccharinate, GLU : Gluconate.

RN	Ligand	$log_{10}K°$ I.S.=0	Reference	Reaction
Am(III) Eu(III)	EDTA	19.67	TDB	$Am^{3+} + Edta^{4-} = Am(Edta)^-$
			This work	$Eu^{3+} + Edta^{4-} = Eu(Edta)^-$
		2.71	Hummel et al., 2005	$Am(Edta)^- + H^+ = Am(HEdta)$
				$Eu(Edta)^- + H^+ = Eu(HEdta)$
	citrate	8.55	TDB	$Am^{3+} + Cit.^{3-} = Am(Cit)_{(aq.)}$
		13.9		$Am^{3+} + 2\ Cit.^{3-} = Am(Cit)_2^{3-}$
		8.55	This work	$Eu^{3+} + Cit.^{3-} = Eu(Cit)_{(aq.)}$
		13.9		$Eu^{3+} + 2\ Cit.^{3-} = Eu(Cit)_2^{3-}$
	α-ISA	-21.5	TDB	$Am^{3+} + H_4ISA^- + (3\text{-}x)\ H_20 = Am(OH)_{3-x}(H_{4-x}ISA)^- + 3H^+$
		-21.4	Tits et al., 2005	
		-8.8 ± 0.3	This work (with hypothesis $\nu(H^+) = +2$)	$Eu^{3+} + H_4ISA^- + (2\text{-}x)\ H_20 = Eu(OH)_{2-x}(H_{4-x}ISA) + 2H^+$
		-16.3 ± 0.3	This work (pH ~ 7.2)	$Am^{3+} + H_4ISA^- = Am(HISA)^- + 3H^+$
		-20.9	TDB	$Eu^{3+} + H_4ISA^- + (3\text{-}x)\ H_20 = Eu(OH)_{3-x}(H_{4-x}ISA)^- + 3H^+$
		-18.2	Van Loon and Glaus, 1998	
		-20.9	Tits et al., 2005 (pH ~ 13.3)	
		-18.5		$Eu^{3+} + H_5GLU^- = Eu(H_2GLU)^- + 3H^+$
		-19.6		$Am^{3+} + H_5GLU^- = Am(H_2GLU)^- + 3H^+$
		*-30.6**	Vercammen et al., 2001*	$Eu^{3+} + H_4ISA^- + (4\text{-}x)\ H_20 = Eu(OH)_{4-x}(H_{4-x}ISA)^{2-} + 4H^+$
		-31.1	Wieland et al., 2002 (with hypothesis $\nu(H^+) = +4$)	
		-28.7		$Eu^{3+} + H_5GLU^- + (4\text{-}x)\ H_20 = Eu(OH)_{4-x}(H_{5-x}GLU)^{2-} + 4H^+$
		-10.97 ± 0.28	Tasi et al., 2018	$Pu^{3+} + H_4ISA^- + H_2O = Pu(OH)(H_3ISA) + 2\ H^+$
	o-phthal.	4.96	TDB	$Eu^{3+} + Phthal.^{2-} = Eu(Phthal.)^+$
		7.34	TDB	$Eu^{3+} + 2\ Phthal.^{2-} = Eu(Phthal.)_2^-$
		4.93	TDB	$Am^{3+} + Phthal.^{2-} = Am(Phthal.)^+$

	succin.	4.36	TDB	$Eu^{3+} + Succin.^{2-} = Eu(Succin.)^{+}$
		6.50	TDB	$Eu^{3+} + 2\ Succin.^{2-} = Eu(Succin.)_2^{-}$
Th(IV)	α-ISA	-5.65	TDB	$Th^{4+} + H_4ISA^{-} + 3\ H_20 = Th(OH)_3(H_4ISA) + 3H^{+}$
		-13.2	TDB	$Th^{4+} + H_4ISA^{-} + 4\ H_20 = Th(OH)_4(H_4ISA)^{-} + 4H^{+}$
		-4.9 -4.9	TDB Rai & Kitamura, 2017	$Th^{4+} + 2\ H_4ISA^{-} + 3\ H_20 = Th(OH)_3(H_4ISA)_2^{-} + 3H^{+}$
		-10.4 -12.5	TDB Rai & Kitamura, 2017	$Th^{4+} + 2\ H_4ISA^{-} + 4\ H_20 = Th(OH)_4(H_4ISA)_2^{2-} + 4H^{+}$
		-9 -10	TDB (gluconate analogy) This work	$Th^{4+} + Ca^{2+} + H_4ISA^{-} + 4\ H_20 =$ $CaTh(OH)_4(H_4ISA)^{+} + 4H^{+}$
		-10.1	Hummel et al., 2005	$Th^{4+} + H_4ISA^{-} = Th(H_4ISA)^{3+}$
		-5.0	Hummel et al., 2005	$Th^{4+} + Ca^{2+} + 2\ H_4ISA^{-} = CaTh(H_2ISA)_2 + 4H^{+}$
		3.2	Rai, 2009	$Th^{4+} + H_4ISA^{-} + H_20 = Th(OH)(H_4ISA)^{2+} + H^{+}$
	citrate	16.8* 13.7	TDB* Hummel et al., 2005	$Th^{4+} + Cit.^{3-} = Th(Cit.)^{+}$
		25.8*	TDB*	$Th^{4+} + 2\ Cit.^{3-} = Th(Cit.)_2^{2-}$
		10.27	Hummel et al., 2005	$Th^{4+} + HCit.^{2-} = Th(HCit.)^{2+}$
		19.24	Hummel et al., 2005	$Th^{4+} + 2\ HCit.^{2-} = Th(HCit.)_2$
Pu(IV) U(IV)		15.3	Hummel et al., 2005	$Pu^{4+} + Cit.^{3-} = Pu(Cit.)^{+}$
		30	Hummel et al., 2005	$Pu^{4+} + 2\ Cit.^{3-} = Pu(Cit.)_2^{2-}$
		11.53	Hummel et al., 2005	$U^{4+} + Cit.^{3-} = U(Cit.)^{+}$
		19.46	Hummel et al., 2005	$U^{4+} + 2\ Cit.^{3-} = U(Cit.)_2^{2-}$
		30	Hummel et al., 2005	$Pu^{4+} + 2\ Cit.^{3-} = Pu(Cit.)_2^{2-}$
U(VI)	Ca^{2+} CO_3^{2-}	27.3 27.2 27.18 27.18 27.0 ± 0.2	Maia, 2018 Shang and Reiller, 2020 Thoenen et al., 2014 TDB Grenthe et al., 2020	$Ca^{2+} + UO_2^{2+} + 3\ CO_3^{2-} = CaUO_2(CO_3)_3^{2-}$
		29.22* 29.8 29.7 30.49 30.7 30.8 ± 0.4	Thoenen et al., 2014 Kalmykov & Choppin, 2009 Maia, 2018 Shang and Reiller, 2020 TDB Grenthe et al., 2020	$2\ Ca^{2+} + UO_2^{2+} + 3\ CO_3^{2-} = Ca_2UO_2(CO_3)_3$
	Mg^{2+} CO_3^{2-}	25.8 26.2 ± 0.2	Maia, 2018 Grenthe et al., 2020	$Mg^{2+} + UO_2^{2+} + 3\ CO_3^{2-} = MgUO_2(CO_3)_3^{2-}$
		27.1 27.1 ± 0.6	Maia, 2018 Grenthe et al., 2020	$2\ Mg^{2+} + UO_2^{2+} + 3\ CO_3^{2-} = Mg_2UO_2(CO_3)_3$
	citrate	8.96	TDB	$UO_2^{2+} + Cit.^{3-} = UO_2(Cit)^{-}$
	α-ISA	3.70	TDB	$UO_2^{2+} + H_4ISA^{-} = UO_2(H_4ISA)^{+}$
		6.60	TDB	$UO_2^{2+} + 2\ H_4ISA^{-} = UO_2(H_4ISA)_2$
	o-phthal.	5.56	TDB	$UO_2^{2+} + Phthal.^{2-} = UO_2(Phthal.)$
	succin.	5.28	TDB	$UO_2^{2+} + Succin.^{2-} = UO_2(Succin.)$

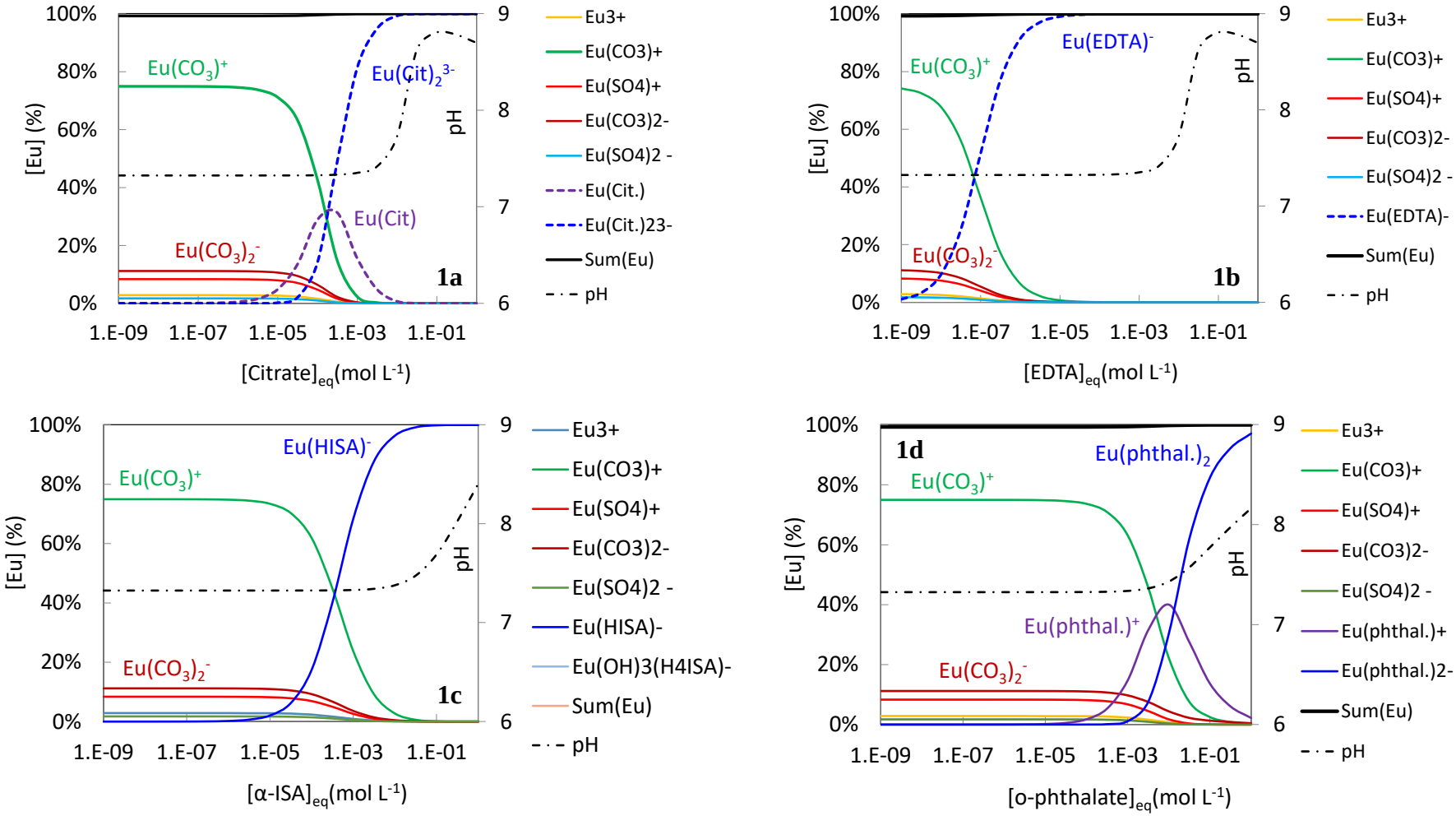

Fig. S1: Speciation of Eu(III) in COx clay rock at equilibrium with citrate (1a), EDTA (1b), α-ISA (1c) or o-phthalate (1d). pH_0 ~7.2, at equilibrium with calcite. ISA complexes proposed by Tits et al. (2005) and this work named arbitrarily $Eu(HISA)^-$ and $Eu(OH)_3(H_4ISA)^-$.

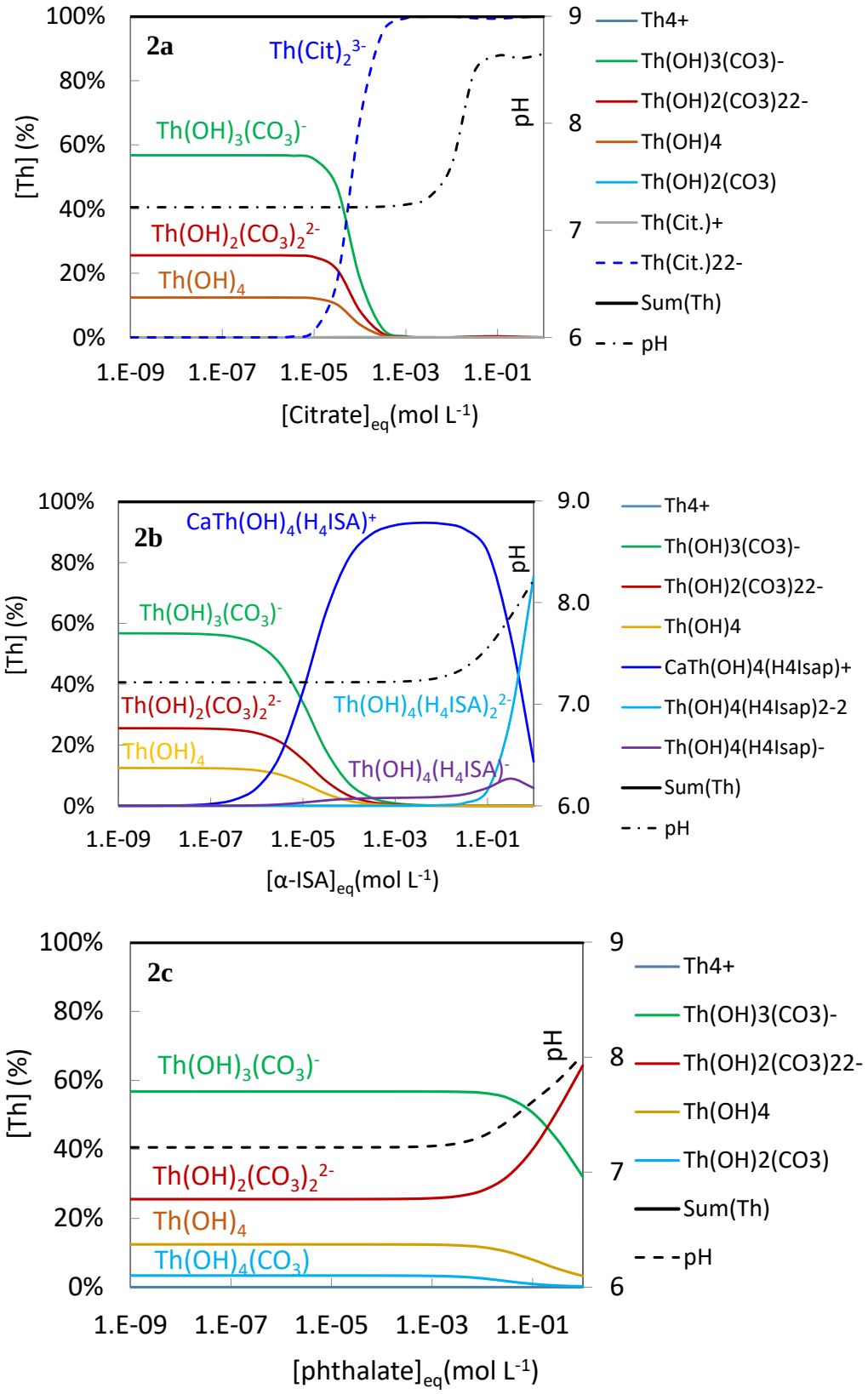

Fig. S2: Speciation of Th(IV) in COx clay rock at equilibrium with citrate (2a), α-ISA (2b) or o-phthalate (2c). pH_0 ~7.2, at equilibrium with calcite.

Bibliography:

Andra, 2005. Dossier 2005 Argile, Synthesis. Evaluation of the Feasibility of a Geological Repository in an Argillaceous Formation. Meuse/Haute-Marne site; Andra Report series 266.

Bradbury, M. H., Baeyens, B., Geckeis, H., Rabung, T., 2005. Sorption of Eu(III)/Cm(III) on Ca-montmorillonite and Na-illite. Part 2: surface complexation modelling. Geochimica et Cosmochimica Acta 69, 5403–5412.

Descostes, M., Tevissen, E., 2004. Definition of an equilibration protocol for batch experiments on Callovo-Oxfordian argillite. Phys. Chem. Earth 29, 79–90.

Descostes, M., Pointeau, I., Radwan, J., Poonoosamy, J., Lacour, J.-L., Menut, D., Vercouter, T., Dagnelie, R.V.H., 2017. Adsorption and retarded diffusion of $Eu^{III}EDTA^{-}$ through hard clay rock. J. Hydrol. 544, 125–132.

Gaucher, E., Robelin, C., Matray, J., Negrel, G., Gros, Y., Heitz, J., Vinsot, A., Rebours, H., Cassagnabère, A., Bouchet, A., 2004. ANDRA underground research laboratory: interpretation of the mineralogical and geochemical data acquired in the Callovo-Oxfordian formation by investigative drilling. Phys. Chem. Earth 29, 55–77.

Grenthe, I., Gaona, X., Plyasunov, A.V., Rao, L., Runde, W.H., Grambow, B., Konings, R.J.M., Smith, A.L., Moore, E.M., 2020. Vol. 14. Second update on the chemical thermodynamics of Uranium, Neptunium, Plutonium, Americium and Technetium, OECD Nuclear Energy Agency Data Bank, Eds., OECD Publications, Paris, France, (2020).

Lerouge, C., Grangeon, S., Gaucher, E.C., Tournassat, C., Agrinier, P., Guerrot, C., Widory, D., Flehoc, C., Wille, G., Ramboz, C., Vinsot, A., Buschaert, S., 2011. Mineralogical and isotopic record of biotic and abiotic diagenesis of the Callovo-Oxfordian clayey formation of Bure (France). Geochem. Cosmochim. Acta 75, 10, 2633–2663.

Pellenard, P., Deconinck, J.-F., 2014. Mineralogical variability of callovo-oxfordian clays from the Paris basin and the subalpine basin. C.R. Geosci. 338, 854–866.

Rasamimanana, S., Lefèvre, G., Dagnelie, R. V. H., 2017. Adsorption of polar organic molecules on sediments: Case-study on Callovian-Oxfordian claystone. Chemosphere 181, 296–303.

Shaw, Paul B., 2013. Studies of the Alkaline Degradation of Cellulose and the Isolation of Isosaccharinic Acids. Doctoral thesis, University of Huddersfield.

Tasi, A., Gaona, X., Fellhauer, D., Böttle, M, Rothe, J., Dardenne, K., Polly, R., Grivé, M., Colàs, E., Bruno, J., Källström, K., Altmaier, M., Geckeis, H., 2018. Applied Geochem. 98, 247–264.

Tits, J., Wieland, E., Bradbury, M.H., Eckert, P., Schaible, A., 2002. The Uptake of Eu(III) and Th(IV) by Calcite Under High pH Cement Pore Water Conditions. PSI Report 02-03, Paul Scherrer Institut, Villigen, Switzerland and Nagra, Technical Report NTB 02-08, Nagra, Wettingen, Switzerland.

Tits, J., Wieland, E., Bradbury, M. H., 2005. The effect of isosaccharinic acid and gluconic acid on the retention of Eu(III), Am(III) and Th(IV) by calcite. Applied Geochem. 20, 2082–2096

Van Loon, L.R., Glaus, M.A., 1998. Experimental and Theoretical Studies on Alkaline Degradation of Cellulose and its Impact on the Sorption of Radionuclides. PSI Report 98-07, Paul Scherrer Institut, Villigen, Switzerland and Nagra Technical Report NTB 97-04, Nagra, Wettingen, Switzerland.

Vercammen, K., Glaus, M.A., Van Loon, L.R., 2001. Complexation of Th(IV) and Eu(III) by α-isosaccharinic acid under alkaline conditions. Radiochim. Acta 89, 393-401.